creative commons
COMMONS DEED

저작자표시-비영리-변경금지 2.0 대한민국

이용자는 아래의 조건을 따르는 경우에 한하여 자유롭게

- 이 저작물을 복제, 배포, 전송, 전시, 공연 및 방송할 수 있습니다.

다음과 같은 조건을 따라야 합니다:

저작자표시. 귀하는 원저작자를 표시하여야 합니다.

비영리. 귀하는 이 저작물을 영리 목적으로 이용할 수 없습니다.

변경금지. 귀하는 이 저작물을 개작, 변형 또는 가공할 수 없습니다.

- 귀하는, 이 저작물의 재이용이나 배포의 경우, 이 저작물에 적용된 이용허락조건을 명확하게 나타내어야 합니다.
- 저작권자로부터 별도의 허가를 받으면 이러한 조건들은 적용되지 않습니다.

저작권법에 따른 이용자의 권리는 위의 내용에 의하여 영향을 받지 않습니다.

이것은 이용허락규약(Legal Code)을 이해하기 쉽게 요약한 것입니다.

Disclaimer

dCollection

이학박사학위논문

염증 반응에서 LSD1의 후성 유전 및 전사 조절 기작에 대한 연구

Studies on the Epigenetic and Transcriptional Regulation of LSD1 in Inflammatory Response

2018년 2월

서울대학교 대학원

생명과학부

김 동 하

Studies on the Epigenetic and Transcriptional Regulation of LSD1 in Inflammatory Response

by

Dongha Kim

Advisor

Professor Sung Hee Baek, Ph.D.

A Thesis for the Degree of Doctor of Philosophy

February, 2018

School of Biological Sciences
Seoul National University

염증 반응에서 LSD1의 후성 유전 및 전사 조절 기작에 대한 연구

Studies on the Epigenetic and Transcriptional Regulation of LSD1 in Inflammatory Response

지도교수 백 성 희

이 논문을 이학 박사 학위논문으로 제출함

2017년 12월

서울대학교 대학원

생명과학부

김동하

김동하의 박사학위논문을 인준함

2017년 12월

위 원 장 원태영 (인)

부 위 원 장 백 성희 (인)

위 원 김준일 (인)

위 원 강찬희 (인)

위 원 김진용 (인)

Studies on the Epigenetic and Transcriptional Regulation of LSD1 in Inflammatory Response

A dissertation submitted in partial fulfillment of the requirement for the degree of

DOCTOR OF PHILOSOPHY

TO THE FACULTY of
THE SCHOOL of BIOLOGICAL SCIENCES
at
SEOUL NATIONAL UNIVERSITY
by

Dongha Kim

Date approved

12/26/17

Tae-Young Yoon

Sunjie Baik

ABSTRACT

Dongha Kim
School of Biological Sciences
The Graduate School
Seoul National University

The inflammatory response is an essential host defense mechanism against invading pathogens. NF-κB signaling plays a key role in regulating the inflammatory response, and misregulation of NF-κB signaling is involved in cancer and autoimmune disease. Although protein kinase C (PKC) signaling is shown to be crucial for the activation of the inflammatory response, the molecular mechanism of activation of the inflammatory response by PKC remains unclear. Here, I find that PKCα is translocated into the nucleus in response to inflammatory signal and directly phosphorylates lysine specific demethylase 1 (LSD1) in the nucleus. Lipopolysaccharide (LPS)-induced LSD1 phosphorylation by PKCα is required for its interaction with p65, and phosphorylated LSD1 facilitates demethylation of p65 leading to enhanced p65 protein stability. Genome-wide analysis reveals that LPS-induced LSD1 phosphorylation leads to activation of NF-κB target genes involved in sepsis. Importantly, *Lsd1*$^{SA/SA}$ mice with ablation of LSD1 phosphorylation show

attenuated LPS-induced lung inflammatory injury and sepsis-induced mortality with greater survival rates than wild-type (WT) mice. Together, our data indicate that targeting PKCα signaling with its downstream LSD1 could be potentially powerful therapeutic strategy for inflammatory diseases such as sepsis.

Key words

Lysine-specific demethylase 1 (LSD1), Protein kinase Cα (PKCα), Phosphorylation, Epigenetic regulation, Nuclear factor-kappa B (NF-κB), p65, CCAAT-enhancer-binding proteins (C/EBPs), Transcription, Lipopolysaccharide (LPS), Inflammation, Sepsis.

Student Number: 2010-20306

CONTENTS

LIST OF FIGURES AND TABLES

CHAPTER I

Introduction

I-1. Lysine-specific demethylase 1 (LSD1)

1.1. Physiological functions of LSD1

Lysine-specific demethylase 1 (LSD1), the first discovered histone demethylase, was belonged to the superfamily of the flavin adenine dinucleotide (FAD)-dependent amine oxidases. LSD1 specifically demethylates mono- or dimethylated histone H3 lysine4 (H3K4) and H3 lysine 9 (H3K9) through formaldehyde-generating oxidation. LSD1 is also acts on several non-histone proteins including HIF-1α, Dnmt1, and E2F1 (Kim et al., 2016; Kontaki and Talianidis, 2010; Wang et al., 2001; Wang et al., 2009; Xiao et al., 2003) (Figure I-1).

LSD1-dependent demethylation of HIF-1α, Dnmt1, and E2F1 regulates the stability of these proteins. LSD1-dependent demethylation of HIF-1α leads to HIF-1α stabilization under hypoxic conditions (Kim et al., 2016). LSD1 also constrains DNA damage induced cell death in the nonexistence of p53 through modulation of the E2F1 (E2F transcription factor 1) protein stability. Demethylation of E2F1 in lysine 185 by LSD1 prevents other E2F adjustments that enterprise E2F degradation, thus preferring E2F gathering once DNA damage occurs (Kontaki and Talianidis, 2010). LSD1 also can remove the methyl group of K1096 residue of DNMT1, the key enzyme in charge of keeping DNA methylation during DNA duplication. In mouse embryonic stem cells (ESCs), LSD1 deficiency results in reduction in DNMT1 protein expressions and an associated damage of overall DNA methylation (Wang et al., 2009).

Recently evidences showed that LSD1 played an important role in a broad spectrum of

biological processes, including cell proliferation (Scoumanne and Chen, 2007), adipogenesis (Musri et al., 2010), spermatogenesis (Myrick et al., 2017), chromosome segregation (Lv et al., 2010) and embryonic development (Foster et al., 2010). Furthermore, LSD1 also could promote progress of tumor by inhibiting the tumor suppressor activity of p53. To date, as a potential drug for discovering anti-tumor drugs, the medical significance of LSD1 inhibitors have been greatly appreciated (Feng et al., 2016).

1.2. Phosphorylation of LSD1

LSD1 is phosphorylated at serine 112 by PKCα kinase *in vivo* and *in vitro*. Knock-in (KI) mice bearing $Lsd1^{SA/SA}$ alleles which are unable to be phosphorylated by PKCα have recently been generated (Nam et al., 2014). $Lsd1^{SA/SA}$ mice bearing phosphorylation-defective $Lsd1^{SA/SA}$ alleles showed altered circadian rhythms and impaired phase resetting of circadian clock.

LSD1 is involved in the regulation of presynaptic gene expression and subsequently regulates the hippocampus-dependent memory in phosphorylation-dependent manner. In addition, short-term synaptic plasticity, such as paired pulse ratio and post-tetanic potentiation was impaired, whereas long-term synaptic plasticity, including long-term potentiation and long-term depression, was normal. Moreover, the frequency of miniature excitatory postsynaptic current was significantly increased, suggesting presynaptic dysfunction in $Lsd1^{SA/SA}$ mice. Interestingly, Short-term and long-term contextual fear memory as well as spatial memory were impaired in $Lsd1^{SA/SA}$ mice (Lim et al., 2017) (Figure I-1). Together, LSD1 phosphorylation plays important roles various brain functions.

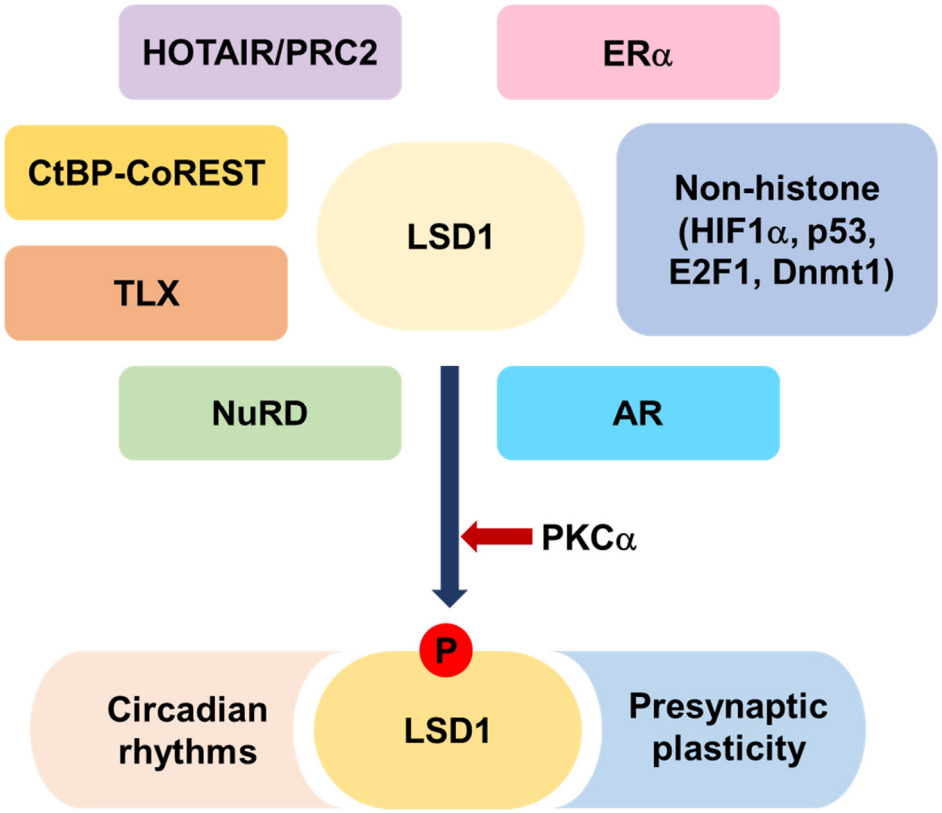

Figure I-1. Illustration of LSD1 functions

LSD1, also known as KDM1A, functions as a transcriptional co-activator or co-repressor in various biological processes. LSD1 is also acts on several non-histone proteins. Phosphorylation of LSD1 by PKCα plays a role of circadian clock and presynaptic plasticity

I-2. Protein kinase Cα (PKCα)

2.1. Structure of PKC family

Protein kinase C (PKC) is a multifunctional, cyclic nucleotide-independent protein kinase that phosphorylates serine and threonine residues in many target proteins. This enzyme was identified in bovine cerebellum as a protein kinase that phosphorylated histone and protamine (Inoue et al., 1977; Nishizuka, 1995; Takai et al., 1977). Since its discovery, much interest has been shown in PKC and its role in signal transduction. Development (Otte et al., 1991), differentiation (Cutler et al., 1993), proliferation (Murray et al., 1993) and carcinogenesis (Ashendel, 1985) all are processes for which PKC has been implicated.

PKC isoforms are members of the PKA, PKG, PKC family of protein kinases that share certain basic structural features. These kinases contain a highly conserved catalytic domain and a regulatory domain that maintains the enzyme in an inactive conformation. PKC regulatory domains reside in the N-terminus of the protein and contain an autoinhibitory pseudosubstrate (PS) domain and two discrete membrane targeting modules, termed C1 and C2. The PKC family can be divided into three subfamilies consisting of conventional PKCs (cPKCs; α, βI/βII and γ isoforms), novel PKCs (nPKCs; δ/θ and ε/η isoforms) and atypical PKCs (aPKCs; ζ and ι/λ isoforms) (Figure I-2). These are known as cPKC isoforms, that require Ca^{2+} and diacylglycerol (DAG) to become activated; nPKC isoforms, that require only DAG; and the aPKC isoforms, that require neither Ca^{2+} nor DAG (Webb et al., 2000).

2.2. Regulations of PKCα

PKC can be activated by calcium and second messenger DAG as serine and threonine specific protein kinases. PKC family members are known to phosphorylate various protein targets and participate in various cell signaling pathways. Each member of the PKC family has a specific expression profile and is considered to play a distinct role in the cell and individual tissue (Bright and Mochly-Rosen, 2005; Griner and Kazanietz, 2007; Liu et al., 2006; Moscat et al., 2006).

PKCα interacts only weakly/transiently with membranes in the absence of calcium or DAG. Agonists that promote phosphoinositide hydrolysis and IP3 generation lead to the mobilization of intracellular calcium, a soluble ligand that binds to the C2 domain and increases its affinity for membranes. This initial electrostatic interaction of the PKCα-C2 domain with membranes is relatively low affinity. However, once anchored to membranes, PKCα diffuses within the plane of the lipid bilayer and participates in a secondary C1A domain interaction with DAG (the membrane-restricted product of phosphoinositide hydrolysis) (Stahelin et al., 2005). Membrane phosphatidylserine (PS) plays a critical role in this secondary membrane interaction, since PS disrupts an electrostatic C1A/C2 interdomain interaction, freeing the C1A domain so that it can penetrate the lipid bilayer and bind DAG (Stahelin et al., 2005). C1A binding to membranes also is relatively low affinity. However, the combined energy from the coordinate C1/C2 domain engagement with membranes leads to high-affinity cPKC binding to membranes and a conformational change that expels the autoinhibitory PS domain from the substrate-binding pocket and facilitates PKC activation (Steinberg, 2008).

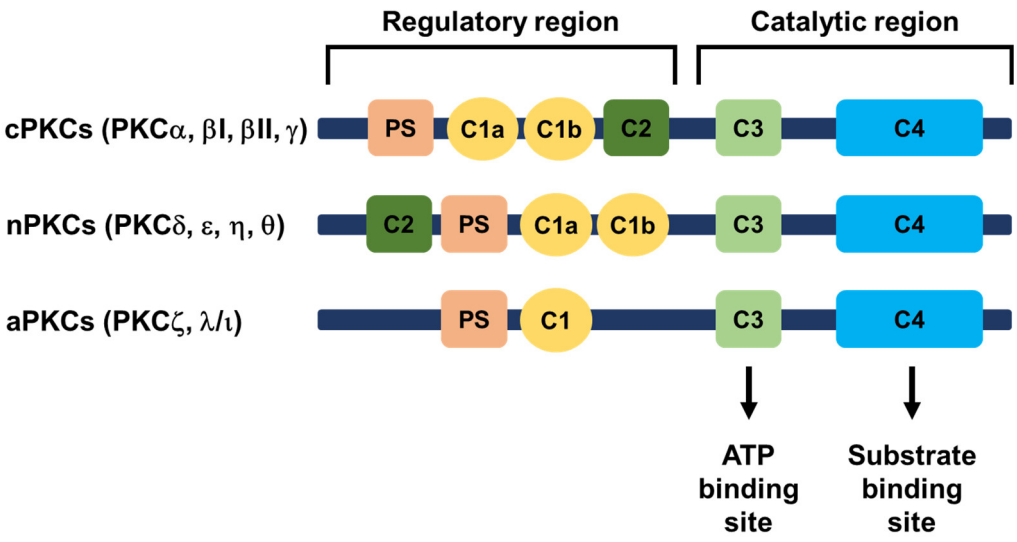

Figure I-2. Classification and structural characteristics of PKC isoforms

Conventional PKC isoforms (cPKCs; α, βI , βII and γ) contain pseudosubstrate domain (PS) and tandem C1a/C1b motifs that bind diacylglycerol (DAG) or phorbol esters (such as PMA) and a C2 domain that binds anionic phospholipids in a calcium-dependent manner.

I-3. Nuclear factor-kappa B (NF-κB)

3.1. Structure of NF-κB family

The NF-κB family of transcription factors consists of NF-κB1 (p50 and its precursor p105), NF-κB2 (p52 and its precursor p100), RelA (also called p65), c-Rel, and RelB, all of which are characterized by presence of an N-terminal Rel homology domain (RHD) responsible for homo- and hetero-dimerization as well as for sequence-specific DNA binding. RelA, c-Rel, and RelB also contain a C-terminal transcription activation domain (TAD), whereas the p52 and p50 subunits do not and therefore rely on interactions with other factors to positively regulate transcription (Wan and Lenardo, 2009).

The NF-κB family members consist of p65/Rel A, p50/NF-κB1, p52, Rel B, and c-Rel (Caamano and Hunter, 2002; Oeckinghaus and Ghosh, 2009). All shares an N-terminal Rel homology region that mediates dimerization, DNA binding, and C-terminal nuclear localization sequence (Muller et al., 1995). The p65-p50 heterodimer is the most abundant and active form. In unstimulated cells, IκB proteins bind to the NF-κB subunits and sequester them in the cytoplasm (Phelps et al., 2000).

3.2. NF-κB signaling pathway

A select set of cell-differentiating or developmental stimuli, such as lymphotoxin-a (LT-a), B-cell activating factor (BAFF) or RANKL, activate the non-canonical NF-κB pathway to induce NF-κB/RelB:p52 dimer in the nucleus. In this pathway, activation of the NF-κB inducing kinase (NIK) upon receptor ligation leads to the phosphorylation and subsequent proteasomal processing of the NF-κB2 precursor protein p100 into mature p52 subunit in a IKK1/IKKα-dependent manner (Basak et al., 2008; Bonizzi et al., 2004; Nelson et al., 2004). Then p52 dimerizes with RelB to appear as a nuclear RelB/p52 DNA binding activity and regulate a distinct class of genes. In contrast to the canonical signaling that relies upon NEMO-IKK2/IKKβ-mediated degradation of IκBα, -β, -ε, the non-canonical signaling critically depends on NIK mediated processing of p100 into p52. Given their distinct regulations, these two pathways were thought to be independent of each other. However, recent studies have revealed that synthesis of the constituents of the non-canonical pathway, RelB and p52, is controlled by the canonical IKK2-IκB-RelA/p50 signaling (Karin, 2008). Moreover, generation of the canonical and non-canonical dimers, vis RelA/p50 and RelB/p52, within the cellular milieu are also mechanistically interlinked. These analyses suggest that an integrated NF-κB system network underlies activation of both RelA and RelB containing dimer and that a malfunctioning canonical pathway will lead to an aberrant cellular response also through the non-canonical pathway (Brasier, 2006; Fusco et al., 2009; Haddad and Abdel-Karim, 2011).

Inflammatory stimulus causes phosphorylation-dependent proteasomal degradation of IκB and liberates NF-κB subunits which translocate from the cytoplasm to the nucleus

(Fuchs et al., 1999; Hatakeyama et al., 1999; Kroll et al., 1999; Wu and Ghosh, 1999; Yaron et al., 1998). The nuclear imported NF-κB subunits bind to κB elements and turn on the expressions of target genes involved in inflammatory responses (Pahl, 1999). The recruitment of co-activators such as CREB binding protein (CBP) is critical for further activation of target genes (Gerritsen et al., 1997; Munshi et al., 1998). In addition, it is known that C/EBPδ acts as an amplifier upon persistent Lipopolysaccharide (LPS) stimulus (Litvak et al., 2009). Persistent LPS treatment induces the gene expression of C/EBPδ by NF-κB, which in turn acts together with NF-κB to further stimulate the transcription of the cytokine-encoding genes (Figure I-3).

3.3. Physiological functions of NF-κB

The canonical pathway plays key roles in the initiation of innate immunity and inflammation responses, as well as the development and maturation of innate and adaptive immune cells (Dev et al., 2011; Hayden et al., 2006). NF-κB is widely used by eukaryotic cells as a regulator of genes that control cell proliferation and cell survival (Brantley et al., 2001; Piva et al., 2006).

NF-κB is a major transcription factor that regulates genes responsible for both the innate and adaptive immune response (Haddad et al., 2002a; Haddad et al., 2002b; Mantovani, 2010). Upon activation of either the T- or B-cell receptor, NF-κB becomes activated through distinct signaling components. Upon ligation of the T-cell receptor, an adaptor molecule, zetachain-associated protein kinase (ZAP70), is recruited via its SH2 domain to the cytoplasmic side of the receptor. ZAP70 helps recruit both lymphocyte-specific protein

tyrosine kinase (LCK) and phosphatidylcholine-specific phospholipase C (PLC-c), which causes the activation of PKC. Through a cascade of phosphorylation events, the kinase complex is activated and NF-κB is able to enter the nucleus to upregulate genes involved in T-cell development, maturation, and proliferation (Brasier, 2006; Haddad et al., 2002a). Because NF-κB controls many genes involved in inflammation, it is not surprising that NF-κB is found to be chronically active in many inflammatory diseases, such as inflammatory bowel disease, arthritis, sepsis, gastritis, asthma, among others (Basak et al., 2007; Bours et al., 1993; Dobrzanski et al., 1995; Jacobs and Harrison, 1998). It is important to note that the key regulators of NF-κB are associated with elevated mortality, especially from cardiovascular diseases (Venuraju et al., 2010). Elevated NF-κB has also been associated with schizophrenia (Haddad and Abdel-Karim, 2011; Song et al., 2009).

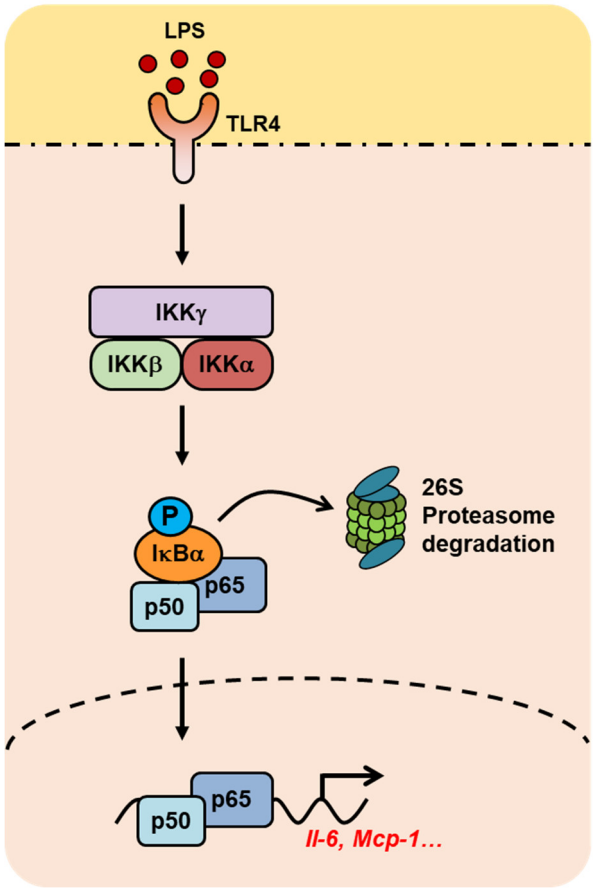

Figure I-3. Illustration of NF-κB signaling pathway

LPS-induced degradation of IκB proteins is initiated through phosphorylation by the IκB kinase (IKK) complex, which consists of two catalytically active kinases, IKKα and IKKβ, and the regulatory subunit IKKγ (NEMO). Phosphorylated IκB proteins are targeted for ubiquitination-dependent proteasomal degradation, which thus releases the bound NF-κB dimers so they can translocate to the nucleus.

I-4. Inflammation

4.1. The function of inflammation

Inflammation is part of the complex biological response of body tissues to harmful stimuli, such as pathogens, damaged cells, or irritants, and is a protective response involving immune cells, blood vessels, and molecular mediators. The function of inflammation is to eliminate the initial cause of cell injury, clear out necrotic cells and tissues damaged from the original insult and the inflammatory process, and initiate tissue repair (Medzhitov, 2008).

Inflammation can be classified as either acute or chronic. Acute inflammation is the initial response of the body to harmful stimuli and is achieved by the increased movement of plasma and leukocytes (especially granulocytes) from the blood into the injured tissues. A series of biochemical events propagates and matures the inflammatory response, involving the local vascular system, the immune system, and various cells within the injured tissue. Prolonged inflammation, known as chronic inflammation, leads to a progressive shift in the type of cells present at the site of inflammation, such as mononuclear cells, and is characterized by simultaneous destruction and healing of the tissue from the inflammatory process (Feghali and Wright, 1997; Ingersoll et al., 2011; Kumar et al., 2004).

4.2. Epigenetic and transcriptional regulation of inflammation

Macrophages play critical roles in diverse chronic diseases, including cancer and allergic responses, and analysis of recent data indicates that chromatin modifications are mechanistically important in the acquisition of the macrophage phenotype (Khansari et al.,

2009). Transcription factors of the NF-κB, FOXP3, IRF, and STAT families along with epigenetic phenomena, including DNA methylation and covalent histone modifications, have been shown to be critical in the regulation of inflammatory genes (Medzhitov (Medzhitov and Horng, 2009). In addition, several of these regulatory factors are controlled by epigenetic mechanisms in T-cells and monocytes (Lal et al., 2009; Wells, 2009; Wierda et al., 2010).

4.3. Septic shock and sepsis

NF-κB signaling needs to be tightly regulated for fine-tuning of the inflammatory response (Ashall et al., 2009; Caldwell et al., 2014); otherwise it may cause systemic inflammatory diseases such as sepsis (Natoli et al., 2011; Semeraro et al., 2012; Smale, 2010). Sepsis is a complex life-threatening response to infection, which leads to tissue damage, organ failure, and death (Semeraro et al., 2012) (Figure I-4). Septic reaction initiates when bacterial products such as endotoxin bind to Toll-like receptors and relay signals through adaptor molecules and transcription factors (TFs) including NF-κB (Abraham, 2003; Akira et al., 2006; Chovatiya and Medzhitov, 2014; Hotchkiss and Opal, 2010; Hotchkiss et al., 1999; Liu and Malik, 2006; Tiruppathi et al., 2014).

In order to understand the mechanism of sepsis and develop effective therapeutic modalities, there is a need to use proper and effective animal models that mimic what occurs in sepsis patients. LPS injection model has been widely used for sepsis (Buras et al., 2005) as it induces systemic inflammation that mimics many of the initial clinical features of sepsis. Together with LPS injection model, the cecal ligation and puncture (CLP) is the

most widely used animal model of sepsis (Buras et al., 2005). The CLP model consists of perforation of the cecum allowing the release of fecal material into the peritoneal cavity to generate immune response induced by poly-microbial infection.

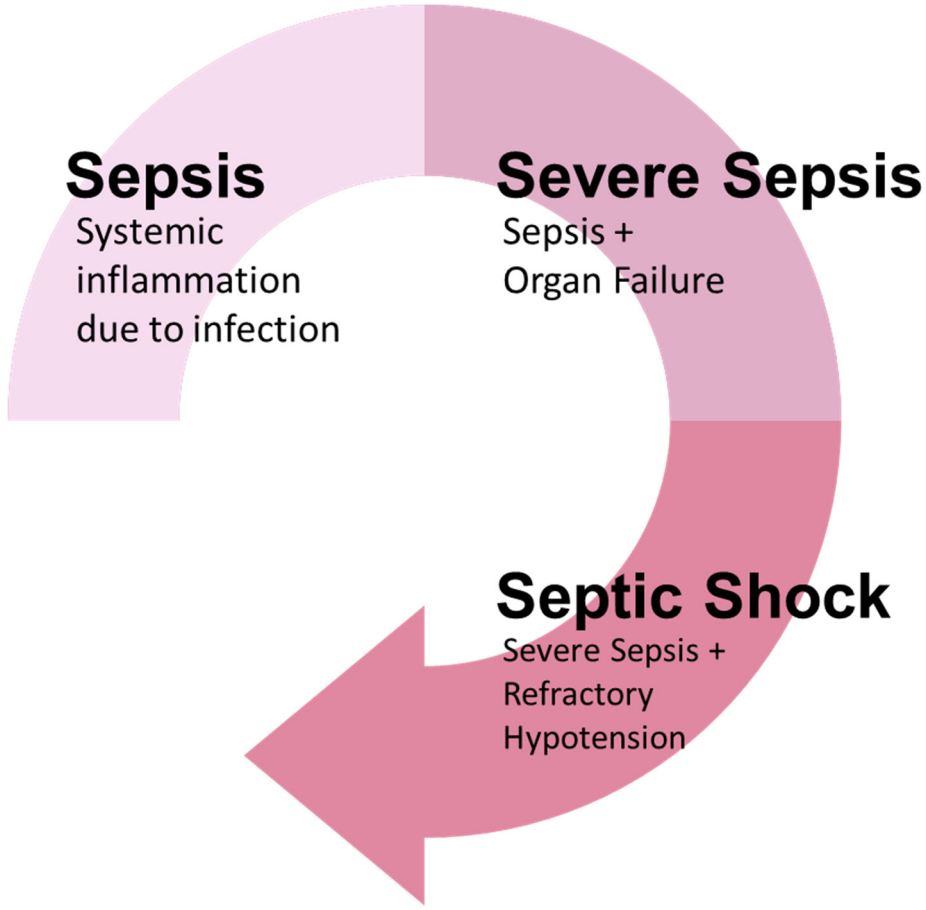

Figure I-4. Illustration of sepsis stages

Sepsis is a life-threatening condition that arises when the body's response to infection causes injury to its own tissues and organs. Severe sepsis is sepsis causing poor organ function or insufficient blood flow. Insufficient blood flow may be evident by low blood pressure, high blood lactate, or low urine output. Septic shock is low blood pressure due to sepsis that does not improve after reasonable amounts of intravenous fluids are given.

CHAPTER II

LSD1 phosphorylation by PKCα is crucial for LPS-induced inflammatory responses

II-1. Summary

Accumulating reports strongly suggest that PKCα is involved in controlling the inflammatory response (Asehnoune et al., 2005; Mackay and Twelves, 2007; Silvan et al., 1996; Wang and Smart, 1999). Application of phorbol 12-myristate 13-acetate (PMA), a classical PKC (PKCα, PKCβ1/β2, and PKCγ) agonist to mice induces acute inflammatory response with increased expressions of the inflammatory cytokines in epidermis (Silvan et al., 1996). Although PKC signaling is shown to be crucial for the activation of inflammatory response (Asehnoune et al., 2005; Langlet et al., 2010), the molecular mechanism of activation of the inflammatory response by PKC including downstream PKC substrates and its target genes remains unclear.

In the previous report, LSD1 is phosphorylated by PKCα on serine 112 site and knock-in mice bearing phosphorylation-defective *Lsd1*$^{SA/SA}$ alleles show altered circadian rhythms and impaired phase resetting (Nam et al., 2014). Given a potential functional link between circadian rhythm and the inflammatory response (Curtis et al., 2014; Scheiermann et al., 2013). Here, I report that PKCα is translocated into the nucleus in response to inflammatory signal leading to LSD1 phosphorylation. Genome-wide analysis reveals that endotoxin-induced LSD1 phosphorylation leads to activation of NF-κB target genes by facilitating p65-p50 heterodimer-mediated transcriptional regulation.

II-2. Introduction

LSD1 is the first reported histone demethylase. In the previous report, LSD1 is also known as AOF2, BHC110, or KDM1A. Due to the restriction of its chemical reactions, LSD1 can only remove mono- or di-methyl groups from proteins. In the initial report, LSD1 was found to target histone H3K4, whose demethylation leads to repression of gene expression (Shi et al., 2004). The follow-up studies have shown that, when associated with androgen receptor (Metzger et al., 2005) or estrogen receptor (Garcia-Bassets et al., 2007), LSD1 can also target histone H3K9, whose demethylation results in activation of gene expression. In addition, LSD1 has been shown to demethylate non-histone proteins, including tumor suppressor p53 (Huang et al., 2007) and DNA methyltransferase-1 (DNMT1) (Wang et al., 2009). Biochemical studies have revealed that LSD1 functions primarily in multi-protein complexes, which includes CtBP1, CoREST, HDAC1/2 and SIRT1 (Lee et al., 2005; Mulligan et al., 2011). LSD1 and its downstream targets are involved in a wide range of biological courses, including embryonic development and tumor-cell growth and metastasis.

Porbol 12-myristate 13-acetate (PMA, also known as TPA) is a protein kinase C agonist commonly used as a chemical stimulator for immune cells. It has been reported that application of PMA to mouse ears induces acute inflammatory response which increases the expression of the inflammatory cytokines in epidermis (Groves et al., 1996). Although there are many clues that PKC signaling pathway is critical for inflammation, little has been known about direct substrates of PKC upon inflammatory signal. Since many studies have provided strong links between circadian rhythms and the immune system, I speculated that

Lsd1$^{SA/SA}$ mice might have defects not only in circadian clock physiology but also in immune response through impaired PKCα-dependent signaling. Here, I identify LSD1 as a critical epigenetic regulator of the inflammatory response. I found that PKCα translocates to the nucleus and phosphorylates LSD1 for further activation with p65 in response to excessive inflammatory stimuli.

II-3. Results

LPS-induced LSD1 phosphorylation by PKCα

Although PKC signaling is shown to be crucial for the activation of inflammatory responses (Asehnoune et al., 2005; Langlet et al., 2010), the molecular mechanism of activation of the inflammatory responses by PKC including downstream PKC substrates and its target genes remains unclear. I prompted to examine whether pro-inflammatory cytokines or endotoxin induce PKCα activation leading to the LSD1 phosphorylation for the regulation of the inflammatory response. Therefore, I treated cells with a variety of pro-inflammatory cytokines or endotoxin and checked the phosphorylation of PKCα and LSD1 in response to cytokine treatment. Among cytokines tested, LPS, TNFα, and IL-1β significantly induced the phosphorylation of PKCα and LSD1 along with p65 translocation in the nuclear fraction of Raw264.7 cells (Figure II-1A). In bone marrow-derived macrophages (BMDMs) obtained from WT mice, LPS treatment led to the phosphorylation of PKCα and LSD1, whereas LSD1 phosphorylation was almost completely abolished in BMDMs obtained from *Lsd1*$^{SA/SA}$ mice (Figure II-1B). Further, LPS-induced LSD1 phosphorylation was detected from lung tissue extracts of WT mice, whereas pre-injection of Go6976, a PKCα inhibitor, completely blocked LSD1 phosphorylation (Figure II-1C).

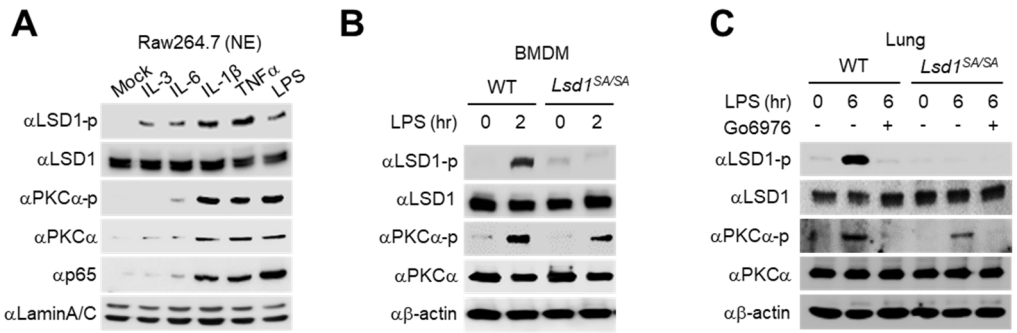

Figure II-1. LPS-induced LSD1 phosphorylation by PKCα

(**A**) Immunoblot analysis was conducted using indicated antibodies in nuclear fraction of Raw264.7 cells after treatment of indicated cytokines and LPS for 2 hours. Lamin A/C was used as a loading control for nuclear proteins. NE (nuclear extract). (**B**) Immunoblot analysis of WT and *Lsd1*$^{SA/SA}$ BMDMs untreated or treated with LPS for 2 hours. (**C**) Immunoblot analysis of lungs from WT and *Lsd1*$^{SA/SA}$ mice (n=6 per group). Mice were intraperitoneally injected with Go6976 (1 mg/kg body weight, dissolved in corn oil) or equal volume of vehicle for 1 hour prior to LPS challenge (10 mg/kg body weight) for 6 hours.

Lsd1$^{SA/SA}$ mice are highly resistant to LPS-induced inflammatory response

To explore whether LSD1 phosphorylation is crucial for the inflammatory response *in vivo*, I first examined whether LPS-induced inflammatory response is impaired in *Lsd1*$^{SA/SA}$ mice. I applied a mouse model of LPS-induced inflammation and acute lung injury using WT and *Lsd1*$^{SA/SA}$ mice. Histopathological examinations revealed that LPS-injected WT mice had severe lung injury and alveolar damage, whereas the response was significantly attenuated in *Lsd1*$^{SA/SA}$ mice (Figure II-2A). In survival studies, 80 % of WT mice died within 66 hours of LPS administration, whereas only 30 % of *Lsd1*$^{SA/SA}$ mice died during the same period (Figure II-2B). I found that the *Lsd1*$^{SA/SA}$ mice are highly resistant to LPS-induced inflammatory response, acute lung injury, and mortality *in vivo*.

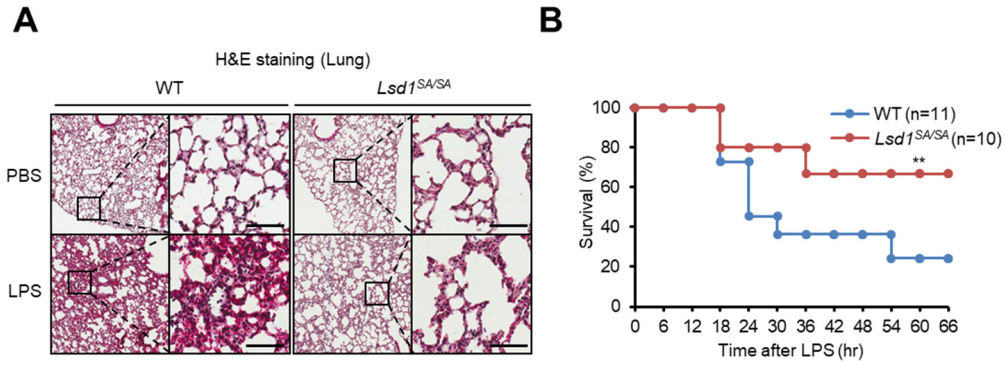

Figure II-2. *Lsd1*$^{SA/SA}$ mice are highly resistant to LPS-induced inflammatory response

(**A**) Representative images of H&E staining of lung sections from WT and *Lsd1*$^{SA/SA}$ mice (n=6 per group) were challenged intraperitoneally with PBS or LPS (10 mg/kg body weight) for 6 hours. Scale bars, 100 μm. Images are representative of three independent experiments. (**B**) Survival of age- and weight-matched male WT (n=11) and *Lsd1*$^{SA/SA}$ (n=10) mice. Mice were challenged with LPS and monitored for 72 hours. **p<0.01 (log-rank test).

LPS induces nuclear translocation of PKCα followed by LSD1 phosphorylation

To explore how LPS induces LSD1 phosphorylation, I conducted immunoblot analysis after subcellular fractionation in primary BMDMs. I found that LPS treatment induced phosphorylation of PKCα, which is active form of PKCα and the phosphorylated PKCα entered the nucleus (Figure II-3A). LPS-induced PKCα translocation to the nucleus is crucial for its interaction with LSD1 as LSD1 bound to PKCα in the nucleus upon LPS treatment, whereas treatment of Go6976 almost completely blocked PKCα translocation to the nucleus leading to the loss of their binding in the nucleus (Figure II-3B). I observed an increase in PKCα phosphorylation concomitant with LSD1 phosphorylation from 60 min of LPS treatment in the nucleus of BMDMs (Figure II-3C) and Raw264.7 macrophage cells (Figure II-3D). Intriguingly, phosphorylation of PKCα and LSD1 was observed in the nuclear fractions of BMDMs (Figure II-3E) and Raw264.7 macrophage cells (Figure II-3F) when treated with high concentration (>100 ng/ml) of LPS. I therefore applied high concentration of LPS in the following experiments to explore the molecular mechanisms of the inflammatory response by LSD1 phosphorylation. Together, I found that only high dose LPS (>100 ng/ml) for over 60 min induces nuclear translocation of PKCα followed by LSD1 phosphorylation in macrophage cells.

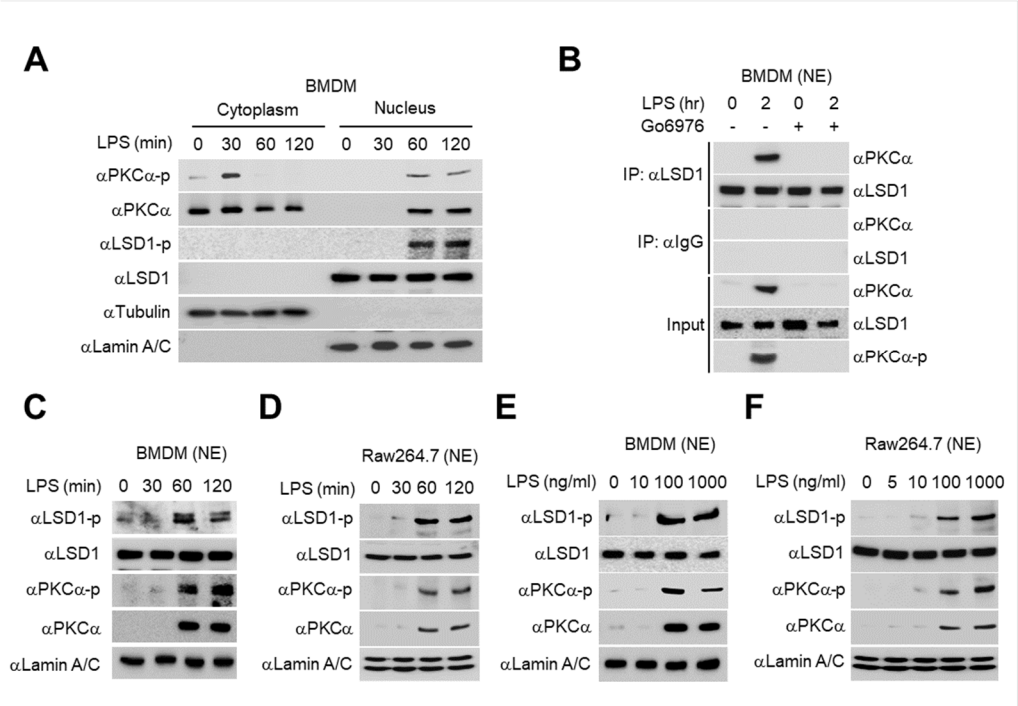

Figure II-3. LPS induces nuclear translocation of PKCα followed by LSD1 phosphorylation

(**A**) Immunoblot analysis of LPS treatment for indicated times before collection in BMDMs. Tubulin was used as a loading control for cytoplasmic proteins. Lamin A/C was used as a loading control for nuclear proteins. (**B**) Co-immunoprecipitation assay of PKCα with LSD1 was conducted in nuclear fraction of BMDMs with LPS treatment for 2 hours in the absence or presence of Go6976 for 6 hours. NE (nuclear extract). (**C** and **D)**) Immunoblot analysis was performed in nuclear fraction of BMDMs (**C**) and Raw264.7 cells (**D**) with LPS treatment for indicated times. (**E** and **F**) Immunoblot analysis using indicated antibodies in nuclear fraction of BMDMs (**E**) and Raw264.7 cells (**F**) after treatment of indicated concentrations of LPS for 2 hours.

Identification of LSD1 phosphorylation target genes by RNA-sequencing analysis

Given that the LPS-induced transcriptional modules are coordinately regulated for signal initiation and amplification of the inflammatory response (Medzhitov and Horng, 2009), I prompted to explore LSD1 phosphorylation-dependent gene sets in transcriptional regulation of the inflammatory response. I performed RNA-sequencing (RNA-seq) experiments in WT and *Lsd1*$^{SA/SA}$ BMDMs following LPS treatment (Figure II-4A). Comparing the transcriptome in WT and *Lsd1*$^{SA/SA}$ BMDMs upon LPS treatment, I identified a total 3,558 differentially expressed genes (DEGs) that can be classified into 6 groups by unsupervised hierarchical cluster analysis (see Materials and Methods) (Figure II-4B).

Among these genes, I was particularly interested in the pools that are activated upon LPS treatment in WT BMDMs but not in *Lsd1*$^{SA/SA}$ BMDMs (Cluster 1), as phosphorylated LSD1 is expected to function as a transcriptional coactivator (Nam et al., 2014). In contrast to genes in other clusters, genes in the Cluster 1 were significantly enriched for p65 peaks around their transcription start site (TSS) (hyper-geometric *p*-value < 1e-130) (Heinz et al., 2013), suggesting that p65 is the major transcription factor (TF) for the induction of genes in Cluster 1 upon LPS treatment (Figure II-4B). Gene ontology (GO) analysis using Enrichr (http://amp.pharm.mssm.edu/Enrichr/) showed that Cluster 1 is enriched for the genes associated with cytokine production and inflammatory response (Figure II-4C and Tables II-1 and II-2). From the global run-on sequencing (GRO-seq) data (Hah et al., 2015), I found that LPS treatment increases the nascent transcript levels from p65 binding sites (-10 kbps ~ -2.5 kbps to TSS) associated with Cluster 1, but not other clusters (Figures II-4D

and II-4E).

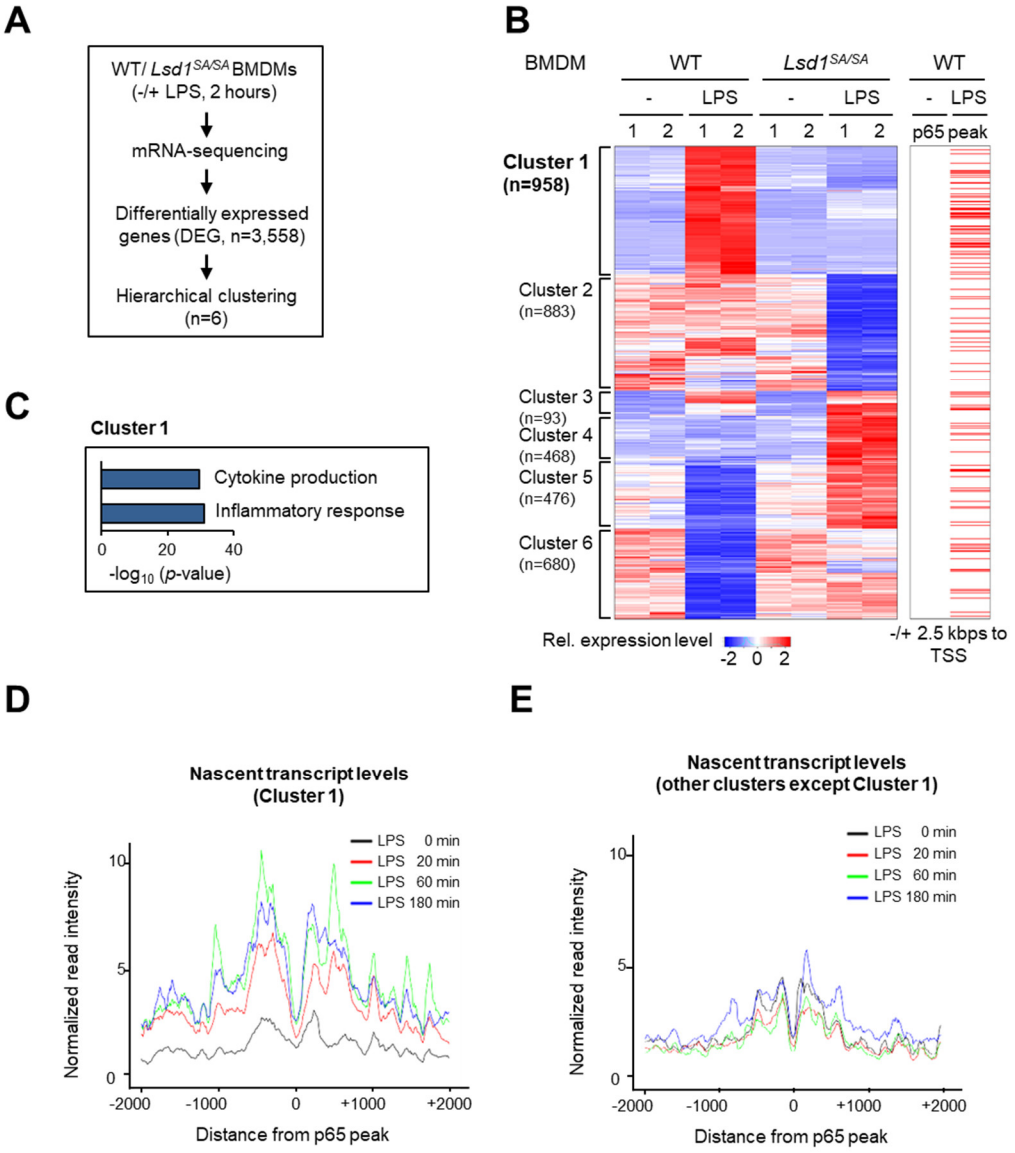
A
WT/ Lsd1SA/SA BMDMs
(-/+ LPS, 2 hours)
mRNA-sequencing
Differentially expressed genes (DEG, n=3,558)
Hierarchical clustering (n=6)
B
BMDM
WT
Lsd1SA/SA
WT
- LPS - LPS - LPS
1 2 1 2 1 2 1 2 p65 peak
Cluster 1 (n=958)
Cluster 2 (n=883)
Cluster 3 (n=93)
Cluster 4 (n=468)
Cluster 5 (n=476)
Cluster 6 (n=680)
Rel. expression level
-2 0 2
-/+ 2.5 kbps to TSS
C
Cluster 1
Cytokine production
Inflammatory response
0 20 40
-log10 (p-value)
D
Nascent transcript levels (Cluster 1)
LPS 0 min
LPS 20 min
LPS 60 min
LPS 180 min
Normalized read intensity
10
5
0
-2000 -1000 0 +1000 +2000
Distance from p65 peak
E
Nascent transcript levels (other clusters except Cluster 1)
LPS 0 min
LPS 20 min
LPS 60 min
LPS 180 min
Normalized read intensity
10
5
0
-2000 -1000 0 +1000 +2000
Distance from p65 peak

Figure II-4. Identification of LSD1 phosphorylation target genes by RNA-sequencing analysis

(**A**) Flow chart showing the strategy of RNA-seq analysis. (**B**) Hierarchical clustering results applied to 3,558 differentially expressed genes (DEGs). The p65 peaks around the TSS (+/- 2.5 kbps) were shown. (**C**) GO analysis for the genes in Cluster 1 showing that cytokine production and inflammatory response genes are significantly enriched in Cluster 1. (**D** and **E**) GRO-seq data after LPS treatment in macrophages are shown around p65 binding sites, and p65 binding sites located within -10 kbps ~ -2.5 kbps from TSS were only considered. LPS treatment increases the nascent transcript levels from p65 binding sites associated with Cluster 1. Nascent transcript levels around p65 binding sites located within -10 kbps ~ -2.5 kbps from TSS in cluster1 (**D**) and other clusters except cluster1 (**E**).

List of cytokine production-related genes (n=99)		
ADAM17	IL23A	REL
ADORA2B	IL27	RELA
BCL10	IL33	RGCC
BCL3	IL6	RIPK2
BCL6	INHBA	RPS6KA5
CCL19	IRAK3	RSAD2
CCL2	IRF1	SEMA7A
CCL3	IRF4	SERPINE1
CD14	IRG1	SPHK1
CD40	JAK2	SRGN
CD74	LAG3	STAT5A
CD80	LRRC32	SYK
CD83	LRRFIP1	TICAM1
CD86	LTB	TICAM2
CEBPB	LTF	TLR1
CLEC4E	MALT1	TLR2
CLEC5A	MAP2K3	TLR6
CSF2	MAPKAPK2	TNF
CX3CL1	MEFV	TNFAIP3
DLL1	MUL1	TNFRSF8
EBI3	MYD88	TNFSF15
FURIN	NFKB1	TNFSF4
FZD5	NFKB2	TNFSF9
HILPDA	NFKBIA	TRAF3
IFIH1	NFKBIB	TREX1
IFNB1	NLRP3	TRPM4
IKBKE	NOD1	XCL1
IL10	NOD2	ZBTB32
IL12A	NOX1	ZC3H12A
IL12B	PDE4B	ZC3HAV1
IL15	PELI1	ZFP36
IL17RA	PTGER4	
IL1A	PTGS2	
IL1B	RABGEF1	

Table II-1. List of cytokine production-related genes

List of cytokine production-related genes in cluster 1 obtained from GO analysis

List of inflammatory response-related genes (n=90)		
ADORA2A	IL23A	S100A8
BCL6	IL27	S100A9
C5AR1	IL2RA	SDC1
CCL19	IL6	SELE
CCL2	IRAK2	SEMA7A
CCL22	IRG1	SGMS1
CCL24	KDM6B	SPHK1
CCL3	KIT	TICAM1
CCL4	MAP2K3	TICAM2
CCL7	MAPKAPK2	TLR1
CCR1	MEFV	TLR2
CCR3	MMP25	TLR6
CCRL2	MYD88	TNF
CD14	NFKB1	TNFAIP3
CD40	NFKBID	TNFAIP6
CEBPB	NFKBIZ	TNFRSF1B
CHI3L1	NLRP3	TNFSF4
CSF1	NOD1	TNIP1
CXCL1	NOS2	TNIP3
CXCL10	NOTCH1	TSPAN2
CXCL11	NOX1	VCAM1
CXCL2	OLR1	XCR1
CXCL3	ORM2	
CYBB	PDPN	
FPR2	PLSCR1	
GJA1	PRDX5	
GPR68	PTGES	
HP	PTGS2	
IL10	PTX3	
IL15	RASGRP1	
IL18RAP	RBPJ	
IL1A	RELA	
IL1B	RIPK2	
IL1RN	RPS6KA5	

Table II-2. List of inflammatory response-related genes

List of inflammatory response-related genes in cluster 1 obtained from GO analysis

LPS-induced LSD1 phosphorylation is required for activation of NF-κB target genes.

As obtained from mRNA-seq analysis (Figure II-4), *De novo* motif analysis also identified p65 as a major TF enriched from Cluster 1 (Figure II-5A). Quantitative RT-PCR analysis of LSD1 phosphorylation-dependent (e. g., *Mcp-1*, *Il-6*, *Il-1β*, and *Cebpd* in Cluster 1) genes in WT and $Lsd1^{SA/SA}$ BMDMs following LPS treatment confirmed the RNA-seq data (Figure II-5B). Further, mRNA levels of LSD1 phosphorylation-dependent genes in Cluster 1 were also significantly attenuated in the lung tissue extracts obtained from LPS-injected $Lsd1^{SA/SA}$ mice compared to those from WT mice (Figure II-5C). Consistently, pre-injection of Go6976 to the WT mice failed to induce mRNA levels of LSD1 phosphorylation-dependent genes in Cluster 1 from lung tissue extracts (Figure II-5D). Together, these data indicate that LPS-induced LSD1 phosphorylation is required for NF-κB target gene activation through p65.

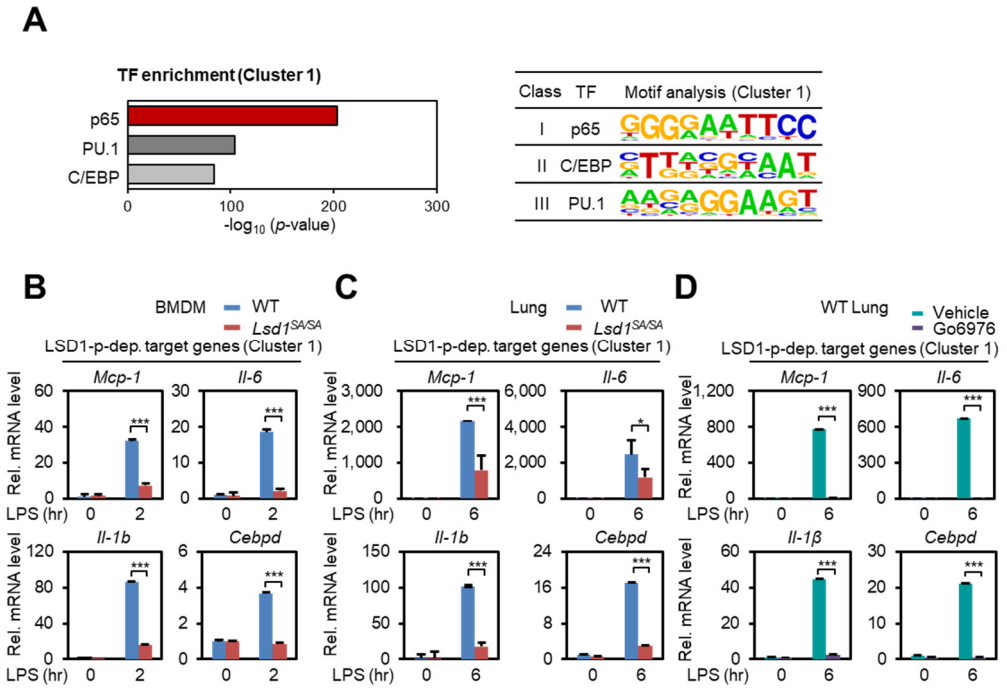

Figure II-5. LPS-induced LSD1 phosphorylation is required for activation of NF-κB target genes.

(**A**) *De novo* motif analysis for the p65 peaks close to the TSSs of the genes in Cluster 1. Hypergeometric *p* values were calculated. (**B**) Quantitative RT-PCR analysis of LSD1 phosphorylation-dependent target genes was conducted using WT or *Lsd1*$^{SA/SA}$ BMDMs untreated or treated with LPS for 2 hours. (**C**) Quantitative RT-PCR analysis of LSD1 phosphorylation-dependent target genes was conducted using lung tissue extracts obtained from vehicle or LPS intraperitoneally injected WT or *Lsd1*$^{SA/SA}$ mice for 6 hours (n=6 per group). (**D**) Quantitative RT-PCR analysis of LSD1 phosphorylation-dependent target genes was conducted using lungs from WT mice (n=6 per group). Mice were intraperitoneally injected with Go6976 (1 mg/kg body weight) or equal volume of vehicle for 1 hour prior to LPS challenge (10 mg/kg body weight) for 6 hours. Data are expressed as Mean ± SD; n=3. *p < 0.05, ***p < 0.001 (Two-way ANOVA).

LPS-induced LSD1 phosphorylation by PKCα is required for its interaction with p65 in the nucleus

As p65 was identified as the major transcription factor regulated by phosphorylated LSD1, I examined whether LSD1 cooperates with p65 in response to LPS. LSD1 interacts with p65 following LPS treatment in nuclear fractions of BMDMs (Figure II-6A). Given that LSD1 is phosphorylated in response to LPS, I speculate that phosphorylated LSD1 binds p65. To check the possibility that PKCα directly phosphorylates p65 as well as LSD1, I performed *in vitro* kinase assay. PKCα failed to phosphorylate p65, suggesting that the direct substrate of PKCα is LSD1, not p65, in LPS-PKCα signaling cascade (Figure II-6B). To find the critical domain of LSD1 to p65 binding or vice versa, I performed *in vitro* GST pull-down assays for domain mapping of p65 and found that 302-427 amino acids of p65, which corresponds to the linker region is critical for LSD1 binding (Figure II-6C). Reciprocally, I performed *in vitro* GST pull-down assays for domain mapping of LSD1. The GST pull-down assay revealed that SWIRM domain of LSD1 possessing PKCα phosphorylation site (S112) is important for the binding to p65 (Figure II-6D).

To examine whether LSD1 phosphorylation is critical for its binding to p65, I performed GST pull-down assay using *in vitro* phosphorylated LSD1. Before the GST pull-down assay, kinase assay using PKCα was conducted to obtain phosphorylated LSD1 form. GST pull-down assay revealed that p65 directly binds phosphorylated LSD1 and treatment of λ-phosphatase almost completely eliminates the binding between LSD1 and p65 (Figure II-6E). Together, these data indicate that LPS-induced LSD1 phosphorylation by PKCα is

required for its interaction with p65 in the nucleus.

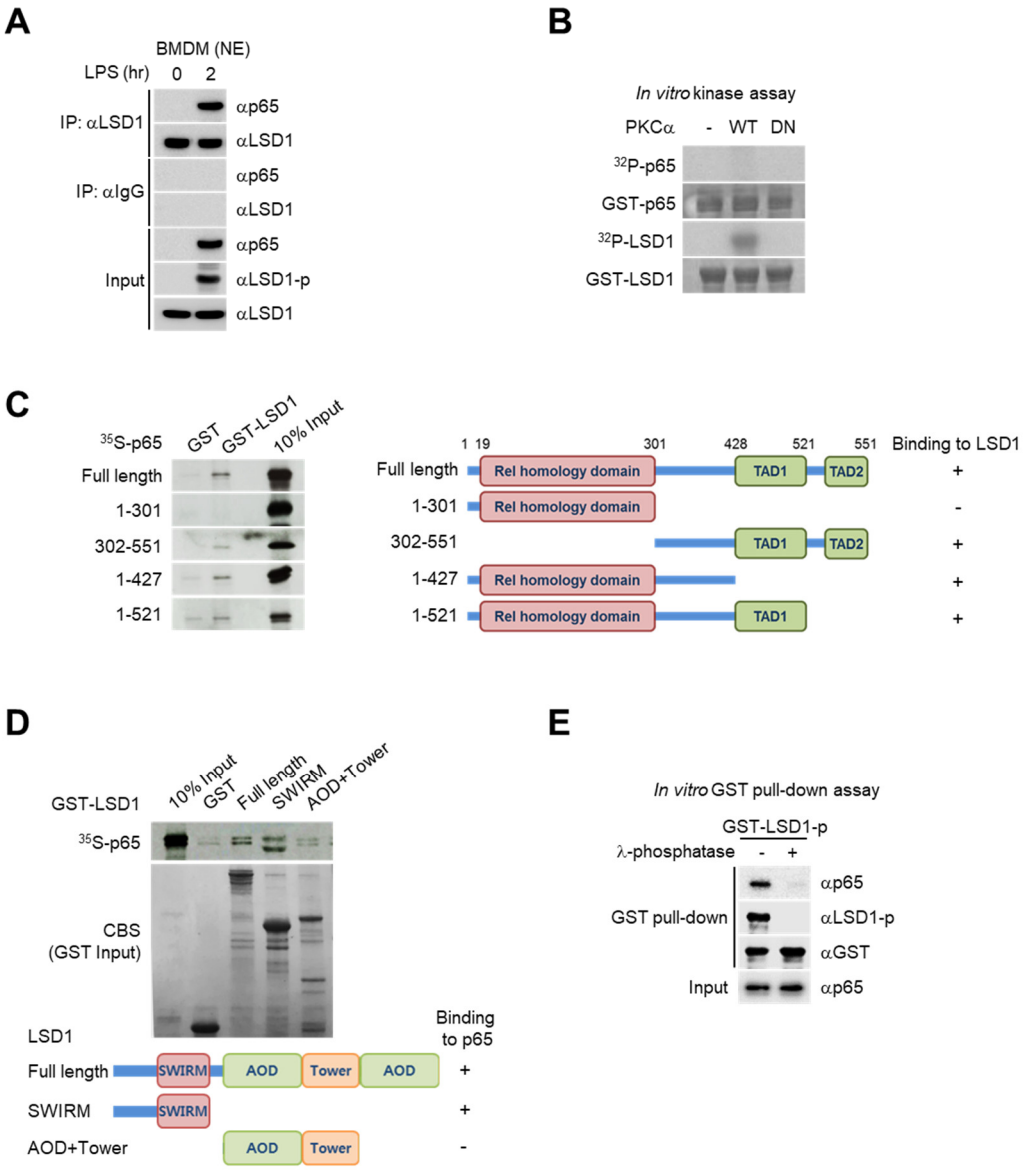
A
BMDM (NE)
LPS (hr) 0 2
IP: αLSD1
αp65
αLSD1
IP: αIgG
αp65
αLSD1
Input
αp65
αLSD1-p
αLSD1
B
In vitro kinase assay
PKCα - WT DN
32P-p65
GST-p65
32P-LSD1
GST-LSD1
C
35S-p65
GST
GST-LSD1
10% Input
Full length
1-301
302-551
1-427
1-521
1 19 301 428 521 551
Binding to LSD1
Full length
Rel homology domain
TAD1
TAD2
+
1-301
Rel homology domain
-
302-551
TAD1
TAD2
+
1-427
Rel homology domain
+
1-521
Rel homology domain
TAD1
+
D
GST-LSD1
10% Input
GST
Full length
SWIRM
AOD+Tower
35S-p65
CBS
(GST Input)
LSD1
Binding to p65
Full length
SWIRM
AOD
Tower
AOD
+
SWIRM
SWIRM
+
AOD+Tower
AOD
Tower
-
E
In vitro GST pull-down assay
GST-LSD1-p
λ-phosphatase - +
GST pull-down
αp65
αLSD1-p
αGST
Input
αp65

Figure II-6. LPS-induced LSD1 phosphorylation by PKCα is required for its interaction with p65 in the nucleus

(**A**) Co-immunoprecipitation assay of p65 with LSD1 was conducted in nuclear fraction of BMDMs untreated or treated with LPS for 2 hours. (**B**) GST-LSD1 and GST-p65 proteins purified from *E. coli* cells were used as substrates for *in vitro* kinase assay using WT or dominant negative mutant (DN) of PKCα. (**C**) *In vitro* GST pull-down assays were conducted using *in vitro*-translated ^{35}S-methionine-labeled p65 full-length or various deletion mutants with phosphorylated GST-LSD1 (kinase assay using PKCα was conducted before GST pulldown) for domain mapping of p65-LSD1 interaction. (**D**) *In vitro* GST pull-down assays were conducted using *in vitro*-translated ^{35}S-methionine-labeled p65 with GST-LSD1 full-length, SWIRM domain mutant, or ASD-Tower domain mutant (kinase assay using PKCα was conducted before GST pulldown) for domain mapping of LSD1-p65 interaction. (**E**) *In vitro* GST pull-down assays were conducted using *in vitro*-translated p65 with phosphorylated GST-LSD1 (kinase assay using PKCα was conducted before GST pull-down assay) in the absence or presence of λ-phosphatase (1,000 units).

LPS-induced LSD1 phosphorylation is required for the recruitment of p65 to target promoters

As obtained from mRNA-seq analysis (Figure II-4), I analyzed *Mcp-1* and *Il-6* promoters as LSD1 phosphorylation-dependent promoters. I performed chromatin immunoprecipitation (ChIP) assay to check whether LSD1 phosphorylation affects the recruitment of LSD1 and p65 to NF-κB target promoters in WT or $Lsd1^{SA/SA}$ BMDMs. ChIP analysis revealed that the recruitments of LSD1 and p65 were significantly increased on *Mcp-1* and *Il-6* promoters in WT BMDMs in response to LPS, but attenuated in $Lsd1^{SA/SA}$ BMDMs (Figure II-7A). To examine whether LPS treatment induces changes in histone methylation status, I checked for histone H3K4 or H3K9 methylation status, which can be regulated by LSD1 (Metzger et al., 2005; Shi et al., 2004). ChIP assays showed comparable H3K4me2, H3K9me2 status on the *Mcp-1* and *Il-6* promoters in WT and $Lsd1^{SA/SA}$ BMDMs, indicating that target gene activation associated with LSD1 phosphorylation in response to LPS is independent of its enzymatic activity as a histone demethylase. On the other hand, histone H3K9 acetylation levels increased in response to LPS on *Mcp-1* and *Il-6* promoters in WT BMDMs, but not in $Lsd1^{SA/SA}$ BMDMs (Figure II-7A). I speculate that the levels of H3K9 acetylation do not increase in $Lsd1^{SA/SA}$ BMDMs following LPS treatment, as p65 fails to be recruited to the target promoters. Furthermore, Go6976 treatment almost completely blocked the recruitment of LSD1 and p65 along with histone H3K9 acetylation to the *Mcp-1* and *Il-6* promoters in Raw264.7 macrophage cells (Figure II-7B). Together, these data indicate that LPS-induced phosphorylation of LSD1 is critical for its binding to

p65 and controls the recruitment of LSD1 and p65 to a subset of NF-κB target promoters.

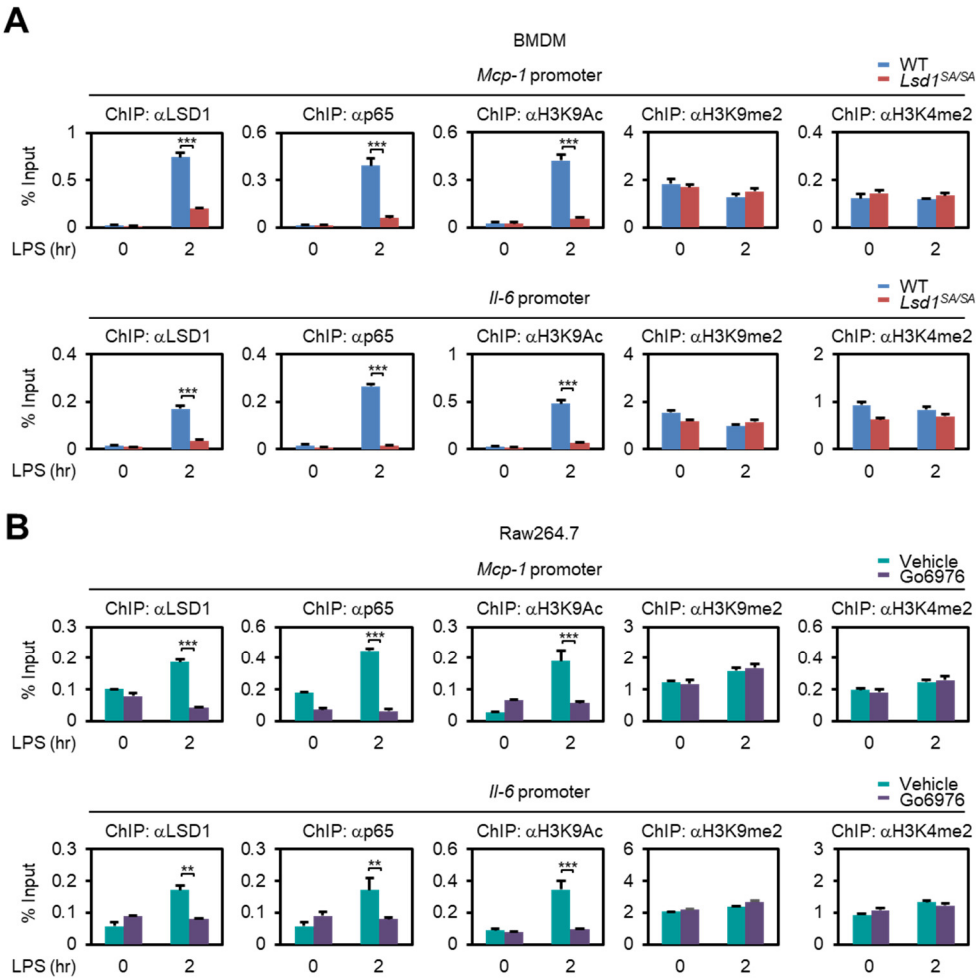

Figure II-7. LPS-induced LSD1 phosphorylation is required for the recruitment of p65 to target promoters

(**A**) ChIP assays on LSD1 phosphorylation-dependent target promoters in WT or *Lsd1*$^{SA/SA}$ BMDMs untreated or treated with LPS for 2 hours. (**B**) ChIP assays on LSD1 phosphorylation-dependent target promoters in Raw264.7 cells pre-treated with Go6976 for 6 hours untreated or treated with LPS for 2 hours. Data are expressed as Mean ± SD; n=3. **p < 0.01, ***p < 0.001 (Two-way ANOVA)

II-4. Discussion

In this study, I identify that PKCα-LSD1-NF-κB signaling cascade operates in response to excessive inflammatory stimuli for the amplification of the inflammatory responses and subsequent development to inflammatory diseases including sepsis. It is important to note that LSD1 phosphorylation-dependent genes in response to high dose of LPS comprise genes involved in sepsis and class II/III TFs (C/EBPδ, C/EBPβ). *Il-6* and *Mcp-1* genes from Cluster 1 are well-known genes involved in sepsis (Deshmane et al., 2009; Rincon, 2012). Interestingly, *Cebpd*$^{-/-}$ mice show attenuated LPS-induced acute lung injury with decreased *Il-6* gene expression compared to WT (Do-Umehara et al., 2013; Yan et al., 2013), a phenotype similar to *Lsd1*$^{SA/SA}$ mice. Induction of *Cebpd* mRNA when PKCα-LSD1-NF-κB signaling cascade operates suggests that this signaling cascade is critical for the subsequent amplification of the inflammatory response, eventually leading to sepsis.

I provide a functional link between excessive inflammatory stimuli and transcriptional and epigenetic regulation of the inflammatory response. Although acute and chronic inflammations induced by PMA, a PKC activator, has been reported (Kontny et al., 2000; Silvan et al., 1996; Wang and Smart, 1999), downstream canonical PKC substrates and its target genes have not been fully understood. Since I found that PKCα enters the nucleus and phosphorylates LSD1 after excessive inflammatory stimuli, it is tempting to speculate that PKCα functions as a sensor that links the cytoplasm and the nucleus and relays external excessive inflammatory stimuli for further activation of the inflammatory response (Figure II-8). Together, the data demonstrate that phosphorylated LSD1 is a key epigenetic factor

for the amplification of the inflammatory response that integrates the inflammatory response and PKC signaling in the nucleus.

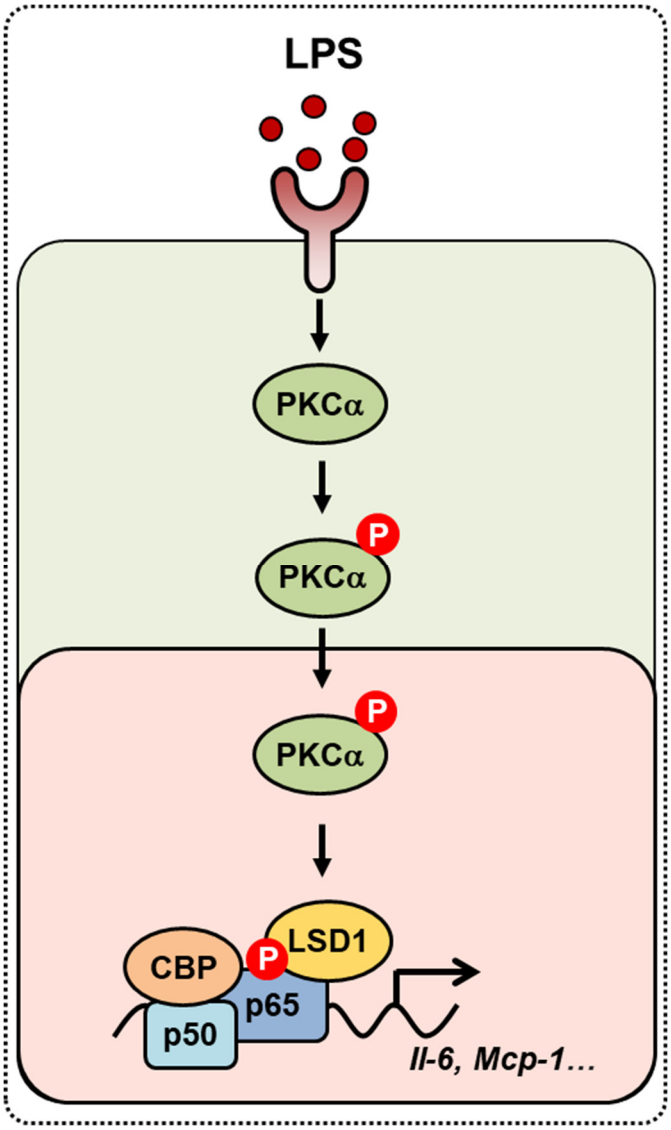

Figure II-8. Schematic model of the LPS-induced PKCα-LSD1-NF-κB signaling cascade

LPS treatment induces nuclear translocation of PKCα followed by LSD1 phosphorylation in the nucleus. LPS-induced LSD1 phosphorylation is crucial for p65 binding for NF-κB target gene activation.

II-5. Materials and Methods

Cell Culture

Raw264.7 (KCLB), MEFs were cultured in Dulbecco's modified Eagle's medium (DMEM, Welgene) supplemented with 10% Fetal Bovine Serum (Gibco) with ZelShield (Minerva Biolabs GmbH). To assure mycoplasma-free conditions, all cells were routinely tested.

Generation of BMDMs

Mice were sacrificed by overexposure to CO_2 anesthesia then femurs and tibias were obtained. After rinsing with 70% ethanol and cold PBS, and bone marrow was isolated from femurs and tibias. Bone marrow cells were plated at a density of 1×10^6 to 2×10^6 cells per ml in RPMI-1640 medium (Welgene) supplemented with 10% FBS (Gibco), ZelShield (Minerva Biolabs GmbH) and macrophage colony stimulating factor (10 ng/ml; Sigma, M9170) on 10 cm petri dishes and were allowed to differentiate for 7-8 days.

Antibodies and reagents

Commercially available antibodies were used: anti-p65 (sc-372, 1:1000 dilution for IB analysis), and anti-LaminA/C (sc-6215, 1:1000 dilution for IB analysis) from Santa Cruz Biotechnology; anti-LSD1 (#2139, 1:1000 dilution for IB analysis), and anti-PKCα (#2056S, 1:1000 dilution for IB analysis) from Cell Signaling; anti-p65 (ab7970), and anti-

LSD1 (ab17721), and anti-H3K9Ac (ab4441), and anti-H3K9me2 (ab1220), and anti-H3K4me2 (ab32356) from abcam; anti-LSD1 (NB-100-1762), and anti-PKCα (NB-110-57356, 1:1000 dilution for IB analysis), and anti-C/EBPδ (NB-110-85519, 1:1000 dilution for IB analysis) from NOVUS; anti-p-PKCα S657 (#06-822, 1:1000 dilution for IB analysis), and anti-p-LSD1 (ABE 1462, 1:200 dilution for IB analysis) from Millipore; anti-HA (MMS-101R, 1:5000 dilution for IB analysis) from Covance; anti-Tubulin (LF-PA0146A, 1:1000 dilution for IB analysis) from Abfrontier; anti-β-actin (A1978, 1:5000 dilution for IB analysis) from Sigma; anti-mono-methyl-p65 (K314/315) (ENH006, 1:500 dilution for IB analysis) from Elabscience Biotechnology; anti-FK2 (BML-PW8810, 1:1000 dilution for IB analysis) from Enzo Life Sciences; Lipopolysaccharides (LPS) from Escherichia coli O127:B8 (L3129), GSK-LSD1 (SML1072) from Sigma; Go6976 (13310) from Cayman; MG132 (M-1157) from A.G. Scientific; TNT T7 Quick Coupled Transcription/ Translation System (L1170) from Promega; λ-phosphatase (P0753) from NEB.

Animals

Lsd1$^{SA/SA}$ mice on the C57BL/6J background have been described (Nam et al., 2014). WT and *Lsd1*$^{SA/SA}$ male mice at 8-10 weeks of age were used in the experiments. Mice were housed under controlled conditions of temperature (22-23°C) and light (12 hours light:12

hours dark, lights switched on at 8:00 AM). Food and water were available *ad libitum*. All animal procedures were approved by the Institutional Animal Care and Use Committee of Seoul National University.

LPS treatment

Cells were serum starved for 24 hours and treated with LPS (1 μg/ml or indicated concentration) for indicated times. Cells were lysed according to the experimental method for immunoblot analysis, quantitative RT-PCR, or ChIP assays.

Quantitative RT-PCR

Total RNA was isolated from lung tissue or BMDMs and Raw264.7 cells using TRIzol (Invitrogen). RNA was reverse-transcribed with oligo (dT) primers and M-MLV Reverse Transcriptase (Enzynomics). The obtained cDNA was mixed with TOPreal™ qPCR 2X PreMIX (SYBR Green with high ROX, Enzynomics) and gene-specific primers for PCR. The abundance of mRNA was detected by an ABI 7500 system with SYBR Green. The following primers were used:

mouse *Mcp-1* Forward 5'-GGCTCAGCCAGATGCAGTTAAC-3',

mouse *Mcp-1* Reverse 5'-AGCCTACTCATTGGGATCATCTTG-3',

mouse *Il-6* Forward 5'-CATAAAATAGTCCTTCCTACCCCAAT-3',

mouse *Il-6* Reverse 5'-CACTCCTTCTGTGACTCCAGCTTA-3',

mouse *Il-1b* Forward 5'-GATGATAACCTGCTGGTGTGTGA-3',

mouse *Il-1b* Reverse 5'-GTTGTTCATCTCGGAGCCTGTAG-3',

mouse *Cebpd* Forward 5'-CTCCACGACTCCTGCCATGT-3',

mouse *Cebpd* Reverse 5'-GAAGAGGTCGGCGAAGAGTTC-3'.

RNA-seq analysis

RNA-seq libraries were prepared using the TruSeq RNA Sample prep kit v2 (Illumina), according to the manufacturer's instructions. RNA-seq libraries were pair-end sequenced on an Illumina Hi-seq 3000/4000 SBS kit v3 (MACROGEN Inc.). All the RNA-seq data were mapped using Tophat package (Kim et al., 2013) against the mouse genome (mm9). Differential analysis has been done via EdgeR package using a false discovery rate (FDR) cut-off of $1x10^{-4}$ (Kim et al., 2013; Robinson et al., 2010). I performed hierarchical clustering analysis using the gene expression values from DEGs. Specifically, I used Ward's criterion for genes with 1 - (correlation coefficient) as a distance measure. Clustering heatmap was drawn using z-score across samples for each gene. ChIP-seq data were mapped to the mouse genome using Bowtie. Peak calling for p65 was performed using the findPeaks command in Homer using the matching input control ChIP-seq data. For each DEGs, I investigated if a p65 peak is located within 10kbps of the TSS. *De novo* motif

finding on the p65 peaks was performed using the findMotifsGenome command in Homer. I used global run-on sequencing (GRO-seq) before and after LPS treatment in macrophage to obtain nascent transcript levels. The GRO-seq fastq files were first trimmed with trim_galore (https://www.bioinformatics.babraham.ac.uk/ projects/trim_galore/) to trimm out the PolA and adaptor sequences (Hah et al., 2015). The trimmed reads were mapped with bowtie (v1.0.0) with the options –best -v 2 -m 1. The bowtie files were then tagged with HOMER's makeTagDirectory function. The average profiles were obtained after normalizing the mapped reads to 1x10-7.

ChIP assays

Cells were cross-linked in 1 % formaldehyde for 10 min and washed with ice-cold PBS two times. Cells were collected into 1ml of harvest buffer (0.1 M Tris-HCl [pH 9.4] and freshly added 10 mM DTT) and incubated for 15 min at 30°C and centrifuged for 3 min at 6000 rpm. Cell pallets were washed sequentially with 1 ml of cold-ice PBS, buffer I (0.25 % Triton X-100, 10 mM EDTA, 10 mM HEPES [pH 6.5], and 0.5 mM EGTA) and buffer II (200 mM NaCl, 1 mM EDTA, 10 mM HEPES [pH 6.5], and 0.5 mM EGTA) and centrifuged for 3 min at 6000 rpm. Chromatin fragmentation was performed by sonication in ChIP lysis buffer (50 mM Tris-HCl [pH 8.1], 1 % SDS, 10 mM EDTA [pH 7.6] and freshly added protease inhibitor cocktail). Chromatin extracts containing DNA fragments

with an average of 250 bp were then diluted ten times with dilution buffer (1 % Triton X-100, 2 mM EDTA, 150 mM NaCl, 20 mM Tris-HCl [pH 8.1] and freshly added protease inhibitor cocktail) and subjected to immunoprecipitations overnight at 4 °C. Immunocomplexes were captured by incubating 40 µl of protein A/G sepharose for 2 h at 4 °C. Beads were washed with TSE I buffer (0.1 % SDS, 1 % Triton X-100, 2 mM EDTA, 20 mM Tris-HCl [pH 8.1] and 150 mM NaCl), TSE II buffer (0.1 % SDS, 1 % Triton X-100, 2 mM EDTA, 20 mM Tris-HCl [pH 8.1] and 500 mM NaCl), buffer III (0.25 M LiCl, 1 % NP-40, 1 % deoxycholate, 10 mM Tris-HCl [pH 8.1] and 1 mM EDTA), three times TE buffer (10 mM Tris-HCl [pH 8.0] and 1 mM EDTA) and eluted in elution buffer (1 % SDS and 0.1 M $NaHCO_3$). Crosslinking was reversed overnight at 65 °C in elution buffer, and DNA was purified with a QIAquick Gel Extraction Kit (QIAGEN). Precipitated DNA was analyzed by quantitative RT-PCR. For quantitative real-time PCR analysis, 2 µl from 50 µl DNA extractions was used. The following primers were used:

mouse *Mcp-1* Forward 5'-CACCCCATTACATCTCTTCCCC-3',

mouse *Mcp-1* Reverse 5'-TGTTTCCCTCTCACTTCACTCTGTC-3',

mouse *Il-6* Forward 5'-AGCTACAGACATCCCCAGTCTC-3',

mouse *Il-6* Reverse 5'-TGTGTGTCGTCTGTCATGCG-3'.

Preparation of tissue lysates

Lungs were rinsed with ice-cold PBS before homogenizing to remove remaining blood. Lungs were homogenized in RIPA lysis buffer (150 mM NaCl, 1 % Triton X-100, 1 % sodium deoxycholate, 0.1 % SDS, 50 mM Tris-HCl [pH 7.5] and 2 mM EDTA [pH 8.0]) freshly supplemented with protease inhibitors. The homogenate was centrifuged (14,000 g at 4°C for 10 min), and cleared supernatant was used for immunoblot analysis.

Whole-cell lysate preparation and subcellular fractionation

All cells were briefly rinsed with ice-cold PBS before collection. For whole-cell lysates, the cells were resuspended in RIPA buffer supplemented with protease inhibitors and sonicated using a Branson Sonifier 450 at output 3 and a duty cycle of 30 for five pulses. For cytosolic and nuclear fractions, cells were lysed in buffer A (10 mM HEPES [pH 7.9], 10 mM KCl, 0.1 mM EDTA, 0.1 mM EGTA and freshly added DTT, PMSF and protease inhibitors), incubated on ice for 15 min and added 0.5 % NP-40, spun at 120 g for 1 min at 4 °C. The supernatant (cytosolic fraction) was transferred to a new tube. The nuclear pellet was rinsed twice with 500 µl of buffer A and spun down at 120 g for 1 min at 4 °C. The supernatant was discarded and the pellet (nuclear fraction) was resuspended in buffer C (20 mM HEPES [pH 7.9], 400 mM NaCl, 1 mM EDTA, 1 mM EGTA and freshly added DTT,

PMSF and protease inhibitors) and sonicated as for the whole-cell lysates. All lysates were quantified by the Bradford method and analyzed by SDS–PAGE.

In vitro kinase assays

In vitro kinase assays using PKCα immunoprecipitated from HEK293T cell lysates as a kinase and purified GST-LSD1 or GST-p65 proteins as substrates were performed. PKCα and GST-LSD1 or GST-p65 were incubated at 30 °C for 30 min in kinase assay buffer (40 mM Tris-HCl [pH 7.5], 10 mM $MgCl_2$, 1 mM DTT, and 5 μCi of [γ-^{32}P] ATP). The reactions were stopped by adding 5X sample buffer and followed by boiling for 10 min. Samples were subjected to SDS-PAGE, and phosphorylation was detected by autoradiography.

In vitro GST pull-down assays

GST fusion constructs were expressed in Rosetta *E. coli* bacteria (Novagen). Crude bacterial lysates were prepared by sonication in GST binding buffer (125 mM NaCl, 20 mM Tris-HCl [pH 7.8], 10 % Glycerol, 0.1 % NP-40, 0.5 mM DTT and freshly added protease inhibitor cocktail) and lysates were centrifuged for 30 min at 13000 rpm. The supernatant was incubated with 100 μl of glutathione-Sepharose beads (GE Healthcare) at 4°C for overnight. p65 protein was generated by adding cold methionine using TNT T7

Quick Coupled Transcription/Translation system (Promega, L1170) according to the manufacture's guidance. *In vitro* kinase assay using cold ATP was performed to generate GST-LSD1 phosphorylation form before GST pull-down assay. After dividing into two tubes, 1000 units of λ-phosphatase (NEB, P0753) were added in either phosphorylated LSD1 and incubated for 30 min at 30°C. Bead bounded GST fusion proteins were washed with buffer (150 mM NaCl, 25 mM Tris-HCl [pH 8.0], 10 % Glycerol, 0.1 % NP-40, and 1 mM EDTA) and mixed with *in vitro* transcribed/translated p65 products in GST binding buffer at 4°C for 1 hour in the presence of the protease inhibitor cocktail. The beads were washed seven times with binding buffer. The reaction beads were boiled for 10 min, then run by SDS-PAGE and analyzed by immunoblot analysis.

Hematoxylin and eosin (H&E) staining

To analyze the phenotypic change of lung in mice, lung samples were removed from each mouse, washed 3 times in PBS to remove remaining blood, fixed in 4% formaldehyde solution (Junsei) in PBS for 20 hours at 4 °C. After fixation, the samples were dehydrated through ethanol series, embedded in paraffin, sectioned into 4 μm sections, and placed on a slide. The slides were deparaffinized in a 60 °C oven, rehydrated, and stained with hematoxylin (Sigma). To remove over-staining, the slides were quick dipped 3 times in 0.3 % acid alcohol, and counterstained with eosin (Sigma). They were then washed in ethanol

series and xylene, and then cover-slipped. Light microscopic analysis of lung specimens was performed by blinded observation to evaluate pulmonary architecture, tissue edema, and infiltration of the inflammatory cells.

Statistical analysis

Data were analyzed by Student's *t*-tests and log rank test for group differences, and by two-way ANOVA for condition and group differences together using GraphPad Prism software. *$p < 0.05$, **$p < 0.01$, ***$p < 0.001$.

CHAPTER III

Demethylation of p65 by LSD1 enhances protein stability of p65

III-1. Summary

Protein methylation has been reported to be involved in protein stability (Hamamoto et al., 2015; Pradhan et al., 2009). SET7/9 is a SET domain-containing methyltransferase that acts on histone H3K4 and on several non-histone proteins including HIF-1α, Dnmt1, and E2F1 (Kim et al., 2016; Kontaki and Talianidis, 2010; Wang et al., 2001; Wang et al., 2009; Xiao et al., 2003). SET7/9-dependent methylations on these proteins are reported to regulate their stability. Similarly, SET7/9 methylates p65 on lysine 314/315 and triggers its degradation (Yang et al., 2009a). LSD1 demethylates H3K4me1/2 or H3K9me1/2 through FAD-dependent amine oxidase reaction (Metzger et al., 2005; Shi et al., 2004). In addition to its role as a histone demethylase, LSD1 plays a prominent role in lysine demethylation of non-histone proteins as a counterpart of SET7/9. SET7/9-mediated methylation of HIF-1α is reversed by LSD1 and LSD1-dependent demethylation of HIF-1α leads to HIF-1α stabilization under hypoxic conditions (Kim et al., 2016). Here, I demonstrate a new signaling axis of PKCα-LSD1-NF-κB in amplification of the inflammatory response following excessive inflammatory stimuli. *Lsd1*$^{SA/SA}$ mice show greater survival rates and attenuated inflammatory cytokines production compared to WT mice under sepsis model. These data indicate that targeting PKCα-LSD1 signaling could be potentially powerful therapeutic strategy for inflammatory diseases such as sepsis.

III-2. Introduction

LSD1 was the first such enzyme identified, which has been shown to demethylate histone H3K4 and H3K9. LSD1 is essential for mammalian development and likely involved in many biological processes. Recent studies show that LSD1 demethylates p53 and Dnmt1 and regulates their cellular functions, indicating that LSD1 fulfills its biological functions by directly acting on both histone and non-histone proteins (Huang et al., 2007; Jin et al., 2013). LSD1 contains several defined domains and associates with a number of protein complexes. Interacting partners of LSD1 may play key roles in determining/modulating the activity and specificity of LSD1 (Nicholson and Chen, 2009; Shi and Whetstine, 2007).

Recent studies indicate that posttranslational modifications of NF-κB, especially of the p65 subunit, play a critical role in fine-tuning the transcriptional activity of NF-κB, adding another important layer of complexity to the transcriptional regulation of NF-κB. In addition to phosphorylation and acetylation, lysine methylation has recently emerged as another important modification for the regulation of nuclear NF-κB function (Chen and Greene, 2004; Neumann and Naumann, 2007; Perkins, 2006). The functional consequence of methylation depends on both position and state of the methylation site, since lysine can be mono-, di-, or tri-methylated. Several methyltransferases have been identified to methylate RelA and regulate distinct functions of NF-κB (Huang et al., 2010).

SET7/9, a SET (suppressor of variegation-enhancer of zeste-trithorax) domain histone lysine methyltransferase, was originally identified to mediate the lysine methylation of

histone H3. Later, many non-histone proteins including p53, estrogen receptors and TAF10, were also found to be targets of SET7/9 (Yang et al., 2009b). SET7/9 specifically monomethylates RelA at K314 and K315 *in vitro* and *in vivo* (Yang et al., 2009a). TNF-α- or LPS-induced methylation of RelA by SET7/9 negatively regulates the function of NF-κB by inducing the ubiquitination and degradation of promoter-bound RelA. Interestingly, in a different study showed that SET7/9 is able to methylate a different lysine residue, K37 (Ea and Baltimore, 2009). In contrast to the negative regulation of NF-κB by SET7/9-mediated methylation of K314 and K315, methylation of K37 appears to be important for the activation of a subset of NF-κB target genes by stabilizing the binding of NF-κB to its enhancers (Ea and Baltimore, 2009). Here, I identify p65 as a new non-histone substrate of LSD1 and thus LSD1 is a substrate of PKCα and functions as a demethylase of p65 leading to enhanced p65 protein stability.

III-3. Results

LSD1 functions as p65 demethylase and phosphorylation of LSD1 is critical in its acquired binding to p65.

Since LSD1 phosphorylation is critical for the proper recruitment of p65 in response to LPS, I focused on the possible role of LSD1 on p65. It has been shown that p65 is methylated by SET7/9 methyltransferase on K314/315 sites and the methylation of p65 triggers its degradation (Yang et al., 2009a). However, the identity of the demethylase responsible for p65 demethylation and subsequent protein stabilization remains unknown. As LSD1 plays a role in demethylation of non-histone proteins as a counterpart of SET7/9 (Kim et al., 2016), I hypothesized that p65 is stabilized through LSD1-mediated demethylation.

To test our hypothesis, I first examined whether LSD1 is responsible for p65 demethylation. Before conducting *in vivo* demethylation assay using enzymatic activity-deficient LSD1 K661A (KA) mutant, I checked whether LSD1 KA mutant affects its binding to p65. LSD1 WT and LSD1 KA mutant exhibited comparable binding to p65 upon LPS treatment, whereas phosphorylation-defective LSD1 S112A (SA) mutant failed to do so (Figure III-1A). I then performed the demethylation assay of p65 and found that the methylation of p65 by SET7/9 was reversed by LSD1 WT, whereas neither SA nor KA mutant of LSD1 were able to reverse p65 methylation (Figure III-1B). Although LSD1 SA mutant possesses comparable demethylase activity to that of WT (Nam et al., 2014), it failed

to demethylate p65 because phosphorylation of LSD1 is required for its binding to p65. I also performed *in vitro* demethylation assay using anti-p65 methylation-specific antibody on K314/315 sites and found that SET7/9-mediated p65 methylation was reversed by phosphorylated form of LSD1 (Figure III-1C). Altogether, these data indicate that in response to LPS, LSD1 functions as p65 demethylase and phosphorylation of LSD1 is critical in its acquired binding to p65.

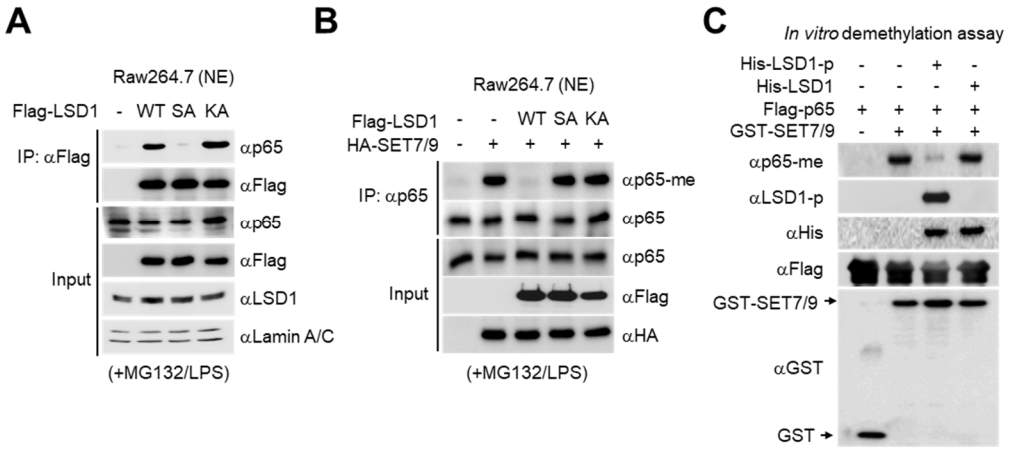

Figure III-1. LSD1 functions as p65 demethylase and phosphorylation of LSD1 is critical in its acquired binding to p65

(**A**) Co-immunoprecipitation assay of p65 with WT, SA or KA mutant of LSD1 in nuclear fraction of Raw264.7 cells transfected with WT, SA or KA mutant of Flag-tagged LSD1 upon MG132 pre-treatment for 4 hours and then LPS treatment for 2 hours. (**B**) *In vivo* demethylation assay was performed in nuclear fraction of Raw264.7 cells upon MG132 pre-treatment for 4 hours and then LPS treatment for 2 hours. After co-immunoprecipitation assay using anti-p65 antibody, the methylated p65 was detected by anti-methyl p65 antibody. (**C**) *In vitro* demethylation assay using Flag-p65 proteins purified from cell lysates as a substrate, GST-SET7/9 proteins purified from *E. coli* as a methyltransferase, and His-LSD1 proteins purified from *E. coli* as a demethylase was performed. *In vitro* kinase assay using PKCα was conducted to obtain phosphorylated LSD1 before demethylation assay. The reaction samples were subject to SDS-PAGE analysis, and methylated p65 was detected by anti-methyl p65 antibody at K314/315 sites.

LSD1 phosphorylation status and LSD1 demethylase activity are critical for p65 protein stability

To clarify whether LSD1 phosphorylation status affects p65 protein stability, I compared nuclear p65 protein levels in WT and *Lsd1*$^{SA/SA}$ BMDMs. Interestingly, nuclear p65 protein levels were not detected in response to LPS in *Lsd1*$^{SA/SA}$ BMDMs, but treatment of MG132, a 26S proteasome inhibitor, restored the nuclear level of p65 in *Lsd1*$^{SA/SA}$ BMDMs (Figure 4D). In addition, I found that recovered p65 proteins by MG132 treatment in the nucleus of *Lsd1*$^{SA/SA}$ BMDMs were methylated form of p65 (Figure III-2A), suggesting that phosphorylated LSD1 is able to bind p65 and blocks methylation-dependent degradation of p65 in the nucleus through its demethylase activity. Ubiquitination assays on p65 were performed to further confirm its regulation. Introduction of LSD1 SA or KA mutant increased p65 ubiquitination in the nucleus, but not in the cytoplasm (Figure III-2B). In parallel, treatment of Go6976 that blocks PKCα activity or GSK-LSD1 that blocks LSD1 activity markedly induced the endogenous ubiquitination of p65 in the nucleus (Figure III-2C). Overall, I provide evidence that both LSD1 phosphorylation status and LSD1 demethylase activity are critical for p65 protein stability (Figure III-2D).

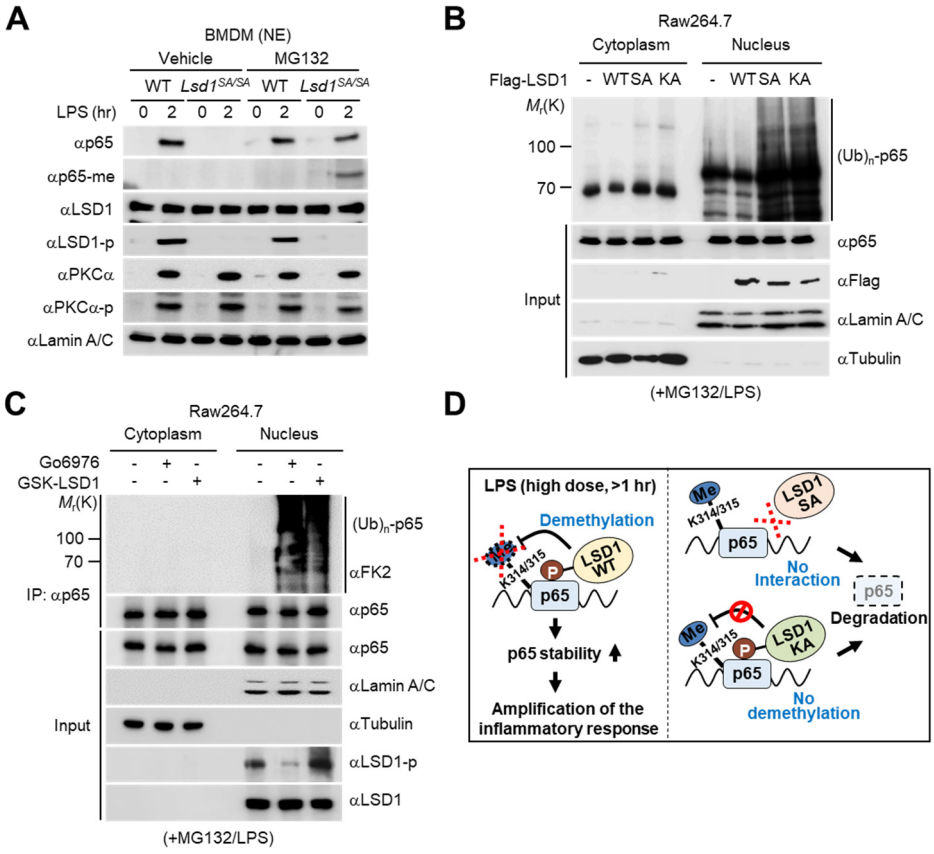

Figure III-2. LSD1 phosphorylation status and LSD1 demethylase activity are critical for p65 protein stability

(**A**) Immunoblot analysis was performed in nuclear fraction of WT and *Lsd1*$^{SA/SA}$ BMDMs with LPS treatment for 2 hours in the absence or presence of MG132 pre-treatment for 4 hours. (**B**) Protein extracts from Raw264.7 cells transfected with WT, SA or KA mutant of Flag-tagged LSD1 upon MG132 pre-treatment for 4 hours and then LPS treatment for 2 hours were subjected to pull-down with Ni^{2+}-NTA beads. Ubiquitination of p65 was assessed by anti-p65 antibody. (**C**) Co-immunoprecipitation assay using anti-p65 antibody in Raw264.7 cells with MG132 pre-treatment for 4 hours and then LPS treatment for 2 hours in the absence or presence of Go6976 or GSK-LSD1 for 6 hours. Ubiquitination of p65 was assessed by anti-FK2 antibody. (**D**) Schematic representation of LSD1 phosphorylation-mediated p65 demethylation resulting in the p65 stabilization.

Enhanced stability of p65 by LSD1 is critical for further activation of inflammatory response genes

It is well established that transcriptional regulations are propagated by sequential cascades of transcription factors (Bolouri and Davidson, 2003; Smith et al., 2007). Induction of the LPS-dependent transcriptional module is orchestrated by many transcription factors (TFs) (Litvak et al., 2009; Medzhitov and Horng, 2009). The class I TFs including NF-κB control the initiation of the inflammatory response within 2 hours of LPS induction. The class II TFs including C/EBPδ are synthesized *de novo* after 2 hours of LPS stimulation and regulate subsequent activation of the inflammatory response genes for signal amplification. The class III TFs including PU.1 and C/EBPβ are lineage-specific transcriptional regulators. All of the TFs function coordinately to control the LPS-induced transcriptional response. From RNA-seq analysis, *de novo* motif analysis validated PU.1 and C/EBP as TFs enriched from Cluster 1 along with p65 (Figure II-5A). Additionally, I identified *Cebpd* as a gene that is induced in LSD1 phosphorylation-dependent manner in Cluster 1.

Since I identified that LSD1 phosphorylation was induced from 60 min following high dose of LPS (Figure II-3), at the critical point where Class I TF and Class II TF can be relayed, I hypothesized that LSD1 phosphorylation regulates subsequent signal activation and amplification of the inflammatory response. Therefore, I analyzed the time course effects of LPS treatment on the expressions of inflammatory response genes in WT and $Lsd1^{SA/SA}$ BMDMs. Interestingly, up to 30 min, there was no significant difference in the induction of *Mcp-1* and *Il-6* mRNA levels between WT and $Lsd1^{SA/SA}$ BMDMs, but later up

to 120 min of LPS treatment, I observed significantly attenuated induction of *Mcp-1* and *Il-6* mRNA levels in *Lsd1*$^{SA/SA}$ BMDMs compared to WT (Figure III-3A). Further, *Cebpd* mRNA expression was significantly attenuated in *Lsd1*$^{SA/SA}$ BMDMs compared to WT from 90 min following LPS treatment (Figure III-3A). Treatment of Go6976 in WT BMDMs prior to LPS treatment showed similar mRNA expression patterns to LPS-treated *Lsd1*$^{SA/SA}$ BMDMs (Figure III-3B). In addition, I found that p65 bound LSD1 from 60 min following LPS treatment, when LSD1 is phosphorylated, suggesting that enhanced stability of p65 by LSD1 is critical for further activation of inflammatory response genes (Figure III-3C).

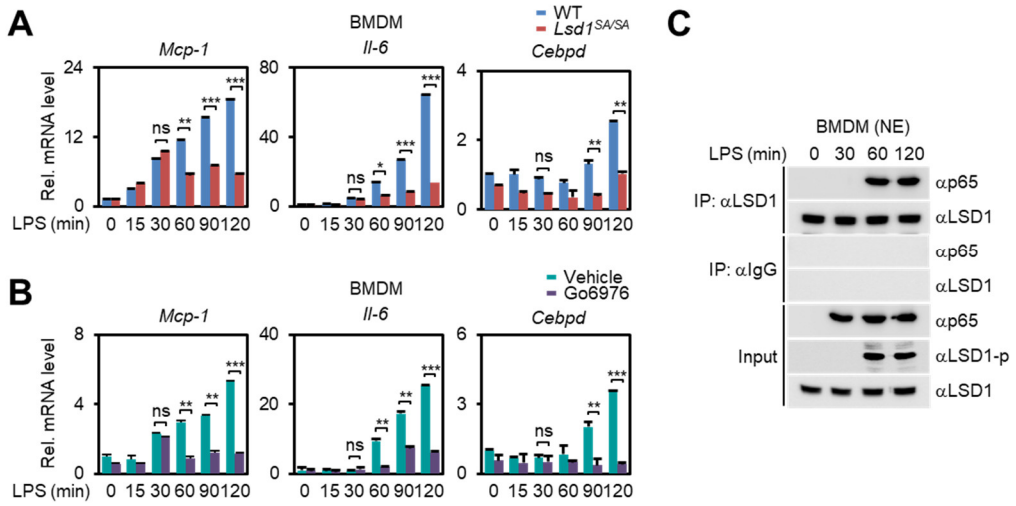

Figure III-3. Enhanced stability of p65 by LSD1 is critical for further activation of inflammatory response genes

(**A**) Quantitative RT-PCR analysis of WT or *Lsd1*$^{SA/SA}$ BMDMs with LPS treatment for indicated times. (**B**) Quantitative RT-PCR analysis of BMDMs with LPS treatment for indicated times in the absence or presence of Go6976 pre-treatment for 6 hours. (**C**) The binding profile of endogenous p65 to LSD1 in nuclear fraction of BMDMs with LPS treatment over an indicated time course. Data are expressed as Mean ± SD; n=3. *p < 0.05, **p < 0.01, ***p < 0.001 (Two-way ANOVA) (**A** and **B**).

LSD1 phosphorylation plays a critical role in the maintenance of p65 recruitment at later time point of LPS treatment

Since C/EBPδ functions as a TF for subsequent activation of the inflammatory response genes, I performed ChIP assay over LPS time course using anti-LSD1, p65, and C/EBPδ antibodies, which allows us to establish the kinetics of promoter occupancy. From 60 min following LPS treatment, LSD1 was recruited on the *Mcp-1* and *Il-6* promoters in WT BMDMs, but failed to be so in $Lsd1^{SA/SA}$ BMDMs (Figure III-4A). Recruitment of p65 to the target promoters was detected in both WT and $Lsd1^{SA/SA}$ BMDMs at 30 min following LPS treatment, as LSD1 is not phosphorylated yet. However, from 60 min following LPS treatment, p65 recruitment was significantly decreased on the *Mcp-1* and *Il-6* promoters in $Lsd1^{SA/SA}$ BMDMs, while maintained, even increased in WT BMDMs (Figure III-4A). These data indicate that LSD1 phosphorylation plays a critical role in the maintenance of p65 recruitment at later time point of LPS treatment. Additionally, C/EBPδ was only recruited at 120 min following LPS treatment in WT BMDMs, which leads to relay and amplification of the inflammatory response (Figure III-4A). In parallel, I obtained similar ChIP results as in $Lsd1^{SA/SA}$ BMDMs with Go6976 treatment (Figure III-4B). Together, these data indicate that PKCα-LSD1-NF-κB signaling cascade operates from 60 min following LPS treatment for the transcriptional activation and subsequent amplification of the inflammatory response genes (Figure III-5).

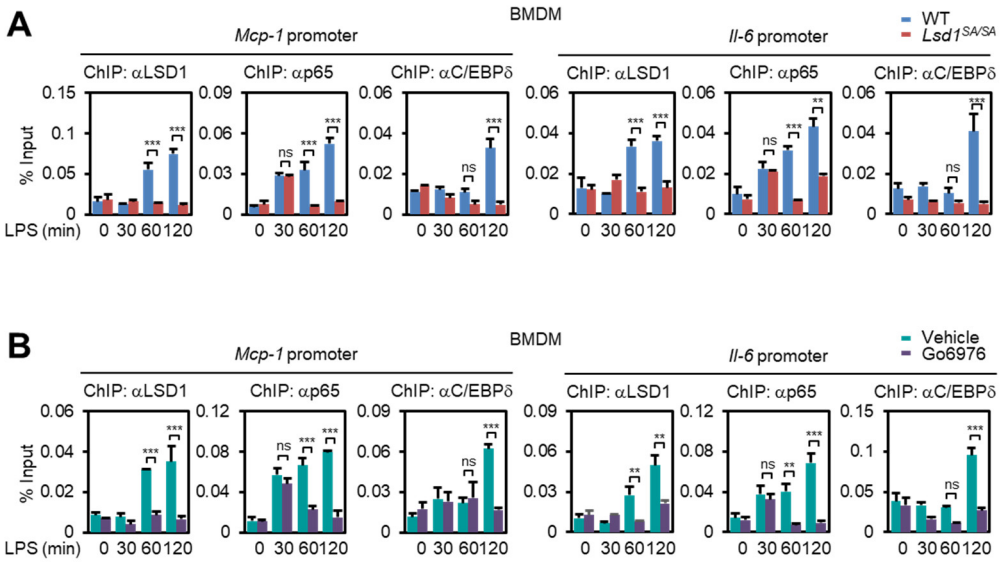

Figure III-4. LSD1 phosphorylation plays a critical role in the maintenance of p65 recruitment at later time point of LPS treatment

(**A**) ChIP assays on LSD1 phosphorylation-dependent target promoters in WT or *Lsd1*$^{SA/SA}$ BMDMs with LPS treatment for indicated times. (**B**) ChIP assays on LSD1 phosphorylation-dependent target promoters in BMDMs. Pre-treatment of Go6976 for 6 hours and then LPS treatment for indicated times before collection. Data are expressed as Mean ± SD; n=3. **p < 0.01, ***p < 0.001 (Two-way ANOVA) (**A** and **B**).

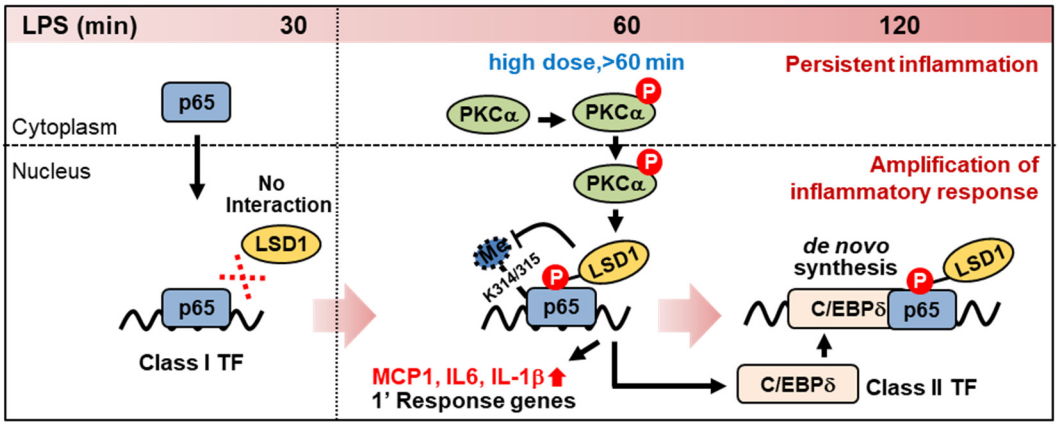

Figure III-5. Schematic of PKCα-LSD1 phosphorylation axis controls the response to prolonged inflammation

PKCα-LSD1-NF-κB signaling cascade operates from 60 min following LPS treatment for the transcriptional activation and subsequent amplification of the inflammatory response genes.

Sustained expression of p65 in the nucleus and subsequent activation of inflammation depends on the PKCα-LSD1-NF-κB signaling cascade

Since I detected reduced recruitment of p65 on the target promoters from 60 min following LPS treatment in *Lsd1*$^{SA/SA}$ BMDMs, I compared the endogenous nuclear p65 protein levels over a time course between WT and *Lsd1*$^{SA/SA}$ BMDMs. LPS-induced p65 translocation to the nucleus was not impaired in *Lsd1*$^{SA/SA}$ BMDMs (Figure III-6A). However, p65 protein levels failed to be maintained in the nucleus along with failure of C/EBPδ *de novo* synthesis at 120 min following LPS treatment in *Lsd1*$^{SA/SA}$ BMDMs (Figure III-6A). Further, immunocytochemistry analysis revealed that p65 stability was comparable in LSD1 WT-, SA-, or KA- reconstituted *Lsd1*$^{-/-}$ mouse embryonic fibroblasts (MEFs) 30 min after LPS treatment. However, at 120 min of LPS treatment, only LSD1 WT-, but nether LSD SA- nor KA mutant-reconstituted *Lsd1*$^{-/-}$ MEFs exhibited stable p65 protein expressions in the nucleus (Figure III-6B). To further confirm that the maintenance of nuclear p65 protein levels and sequential *de novo* synthesis of C/EBPδ are dependent of PKCα-LSD1 signaling axis, immunoblot analysis was performed in nuclear fraction treated with Go6976 or GSK-LSD1. Treatment of Go6976 or GSK-LSD1 failed to stabilize p65 from 60 min following LPS treatment in WT BMDMs (Figure III-6C) or in Raw264.7 cells (Figure III-6D). Furthermore, treatment of MG132 restored the degradation of nuclear p65 proteins caused by Go6976 or GSK-LSD1 (Figure III-6E). Together, these data indicate that PKCα-LSD1-NF-κB signaling cascade is critical to prolonged inflammation for the maintenance of nuclear p65 and sequential *de novo* synthesis of C/EBPδ.

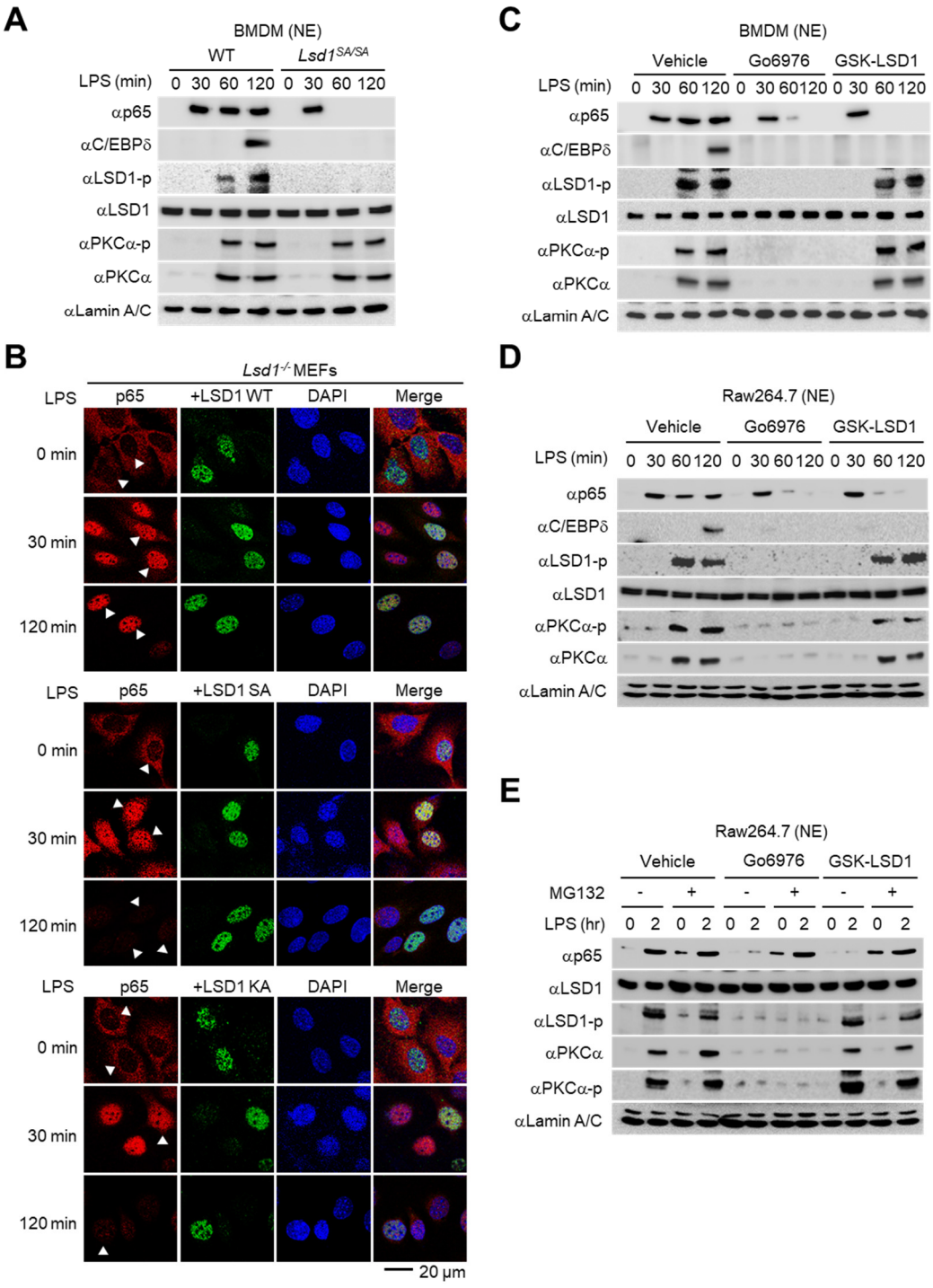
A
BMDM (NE)
WT
Lsd1SA/SA
LPS (min)
0 30 60 120 0 30 60 120
αp65
αC/EBPδ
αLSD1-p
αLSD1
αPKCα-p
αPKCα
αLamin A/C
B
Lsd1-/- MEFs
LPS
p65
+LSD1 WT
DAPI
Merge
0 min
30 min
120 min
LPS
p65
+LSD1 SA
DAPI
Merge
0 min
30 min
120 min
LPS
p65
+LSD1 KA
DAPI
Merge
0 min
30 min
120 min
20 μm
C
BMDM (NE)
Vehicle
Go6976
GSK-LSD1
LPS (min)
0 30 60 120 0 30 60120 0 30 60 120
αp65
αC/EBPδ
αLSD1-p
αLSD1
αPKCα-p
αPKCα
αLamin A/C
D
Raw264.7 (NE)
Vehicle
Go6976
GSK-LSD1
LPS (min)
0 30 60 120 0 30 60 120 0 30 60 120
αp65
αC/EBPδ
αLSD1-p
αLSD1
αPKCα-p
αPKCα
αLamin A/C
E
Raw264.7 (NE)
Vehicle
Go6976
GSK-LSD1
MG132
- + - + - +
LPS (hr)
0 2 0 2 0 2 0 2 0 2 0 2
αp65
αLSD1
αLSD1-p
αPKCα
αPKCα-p
αLamin A/C

Figure III-6. Sustained expression of p65 in the nucleus and subsequent activation of inflammation depends on the PKCα-LSD1-NF-κB signaling cascade

(**A**) Immunoblot analysis was performed in nuclear fraction of WT and *Lsd1*$^{SA/SA}$ BMDMs with LPS treatment for indicated times. (**B**) Representative confocal images of immunocytochemistry. Immunocytochemistry assay was performed in *Lsd1*$^{-/-}$ MEFs reconstituted with WT, SA or KA mutant of HA-tagged LSD1 treated with LPS for indicated times. HA (green); p65 (red); DAPI (blue). Scale bar, 20 μm. (**C** and **D**) Immunoblot analysis was performed in nuclear fraction of BMDMs (**C**) and Raw264.7 cells (**D**). Pre-treatment of Go6976 or GSK-LSD1 for 6 hours followed by LPS treatment for indicated times before collection. (**E**) Immunoblot analysis was performed in nuclear fraction of Raw264.7 cells. Go6976 or GSK-LSD1 is pre-treated for 6 hours followed by LPS treatment for 2 hours in the absence or presence of MG132 for 4 hours.

Inhibition of PKCα or LSD1 activity increased survival rates in CLP-induced sepsis model

To investigate the *in vivo* effects of Go6976 or GSK-LSD1, I injected Go6976 or GSK-LSD1 to mice and performed immunoblot analysis of nuclear fractions from lung tissues. Go6976 or GSK-LSD1-injection failed to stabilize p65 and synthesize C/EBPδ *de novo* in response to LPS (Figure III-7A). As LPS-induced systemic inflammation was much lower in $Lsd1^{SA/SA}$ mice than WT counterparts (Figures II-2A and II-2B), I aimed to confirm our findings in a severe sepsis mouse model. LPS injection and the cecal ligation and puncture (CLP) are widely used to mimic severe sepsis in mice (Buras et al., 2005) (Figure III-8). While LPS injection induces systemic inflammation that mimics many of the initial clinical features of sepsis, the CLP-induced sepsis model shows a cytokine profile similar to that in human sepsis by allowing the release of fecal material into the peritoneal cavity to generate immune response (Buras et al., 2005; Wang et al., 2004).

I used CLP to induce polymicrobial sepsis in age-, sex-, and weight-matched WT and $Lsd1^{SA/SA}$ mice. Intriguingly, I noted 100 % mortality in WT mice within 90 hours of CLP, whereas only 50 % of $Lsd1^{SA/SA}$ mice died during the same period and were alive for more than 144 hours after CLP (Figure III-7B). Next, I checked the possibility that blocking PKCα or LSD1 activity would diminish mortality and attenuate lung injury. I assessed the survival rates of WT mice administered with Go6976, GSK-LSD1, or equal volume of vehicle twice, at 12 hours and 50 hours after CLP challenge. I noted 100 % mortality in vehicle-injected mice within 78 hours of CLP, whereas only 40 % of Go6976-injected mice

and 50 % of GSK-LSD1-injected mice died during the same period and these mice were alive for more than 144 hours after CLP (Figures III-7C and III-7D). Consistent with these data, histopathological examinations showed that WT mice had severe lung injury and alveolar damage after CLP, whereas those responses were significantly reduced in Go6976- or GSK-LSD1-injected mice as in *Lsd1*$^{SA/SA}$ mice (Figure III-7E). Together, these data indicated that Go6976- or GSK-LSD1-injected mice are highly resistant to CLP-induced septic shock.

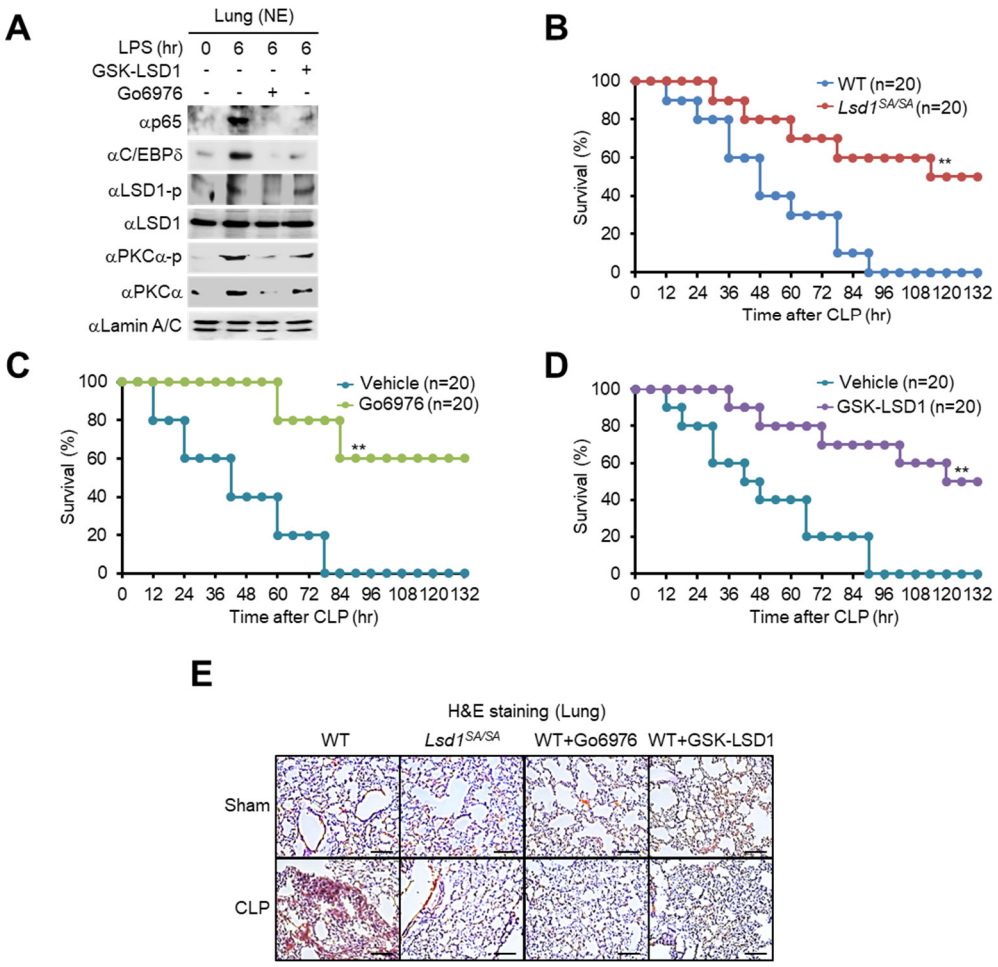

Figure III-7. Inhibition of PKCα or LSD1 activity increased survival rates in cecal ligation and puncture (CLP)-induced sepsis model

(**A**) Immunoblot analysis of lungs from WT mice (n=3 per group). Mice were intraperitoneally injected with Go6976 (1 mg/kg body weight), GSK-LSD1 (1 mg/kg body weight) or equal volume of vehicle for 1 hour prior to LPS challenge (10 mg/kg body weight) for 6 hours. (**B**) WT (blue line) or *Lsd1*$^{SA/SA}$ (red line) mice were subjected to CLP (n=20 each). Animal survival was monitored every 6 hours for 144 hours after CLP. (**C** and **D**) WT mice (n=20) were administered with Go6976 (green line) or equal volume of vehicle

(blue line) (**C**) or GSK-LSD1 (purple line) or equal volume of vehicle (blue line) (**D**) after CLP (1 mg/kg body weight, each, i.v., at 12 hours and 50 hours after CLP). Animal survival was monitored every 6 hours for 144 hours after CLP. **$p < 0.01$ (log-rank test) (**B**-**D**). (**E**) Representative images of H&E staining of lung sections from WT and *Lsd1*$^{SA/SA}$ mice after CLP (n=6 per group) or from WT mice intravenously injected with Go6976, GSK-LSD1, or vehicle (n=6 per group, 1 mg/kg body weight, at 12 hours and 50 hours after CLP). Mice were euthanized 72 hours after CLP. Scale bars, 200 μm.

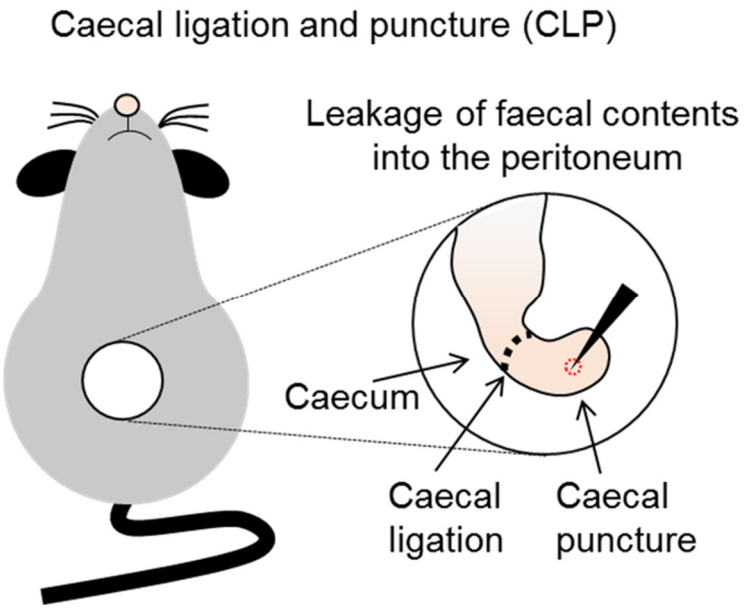

Figure III-8. Illustration of CLP-induced sepsis model

The CLP model consists of perforation of the cecum allowing the release of fecal material into the peritoneal cavity to generate immune response induced by poly-microbial infection.

$Lsd1^{SA/SA}$ mice, Go6976-injected or GSK-LSD1-injected mice were reduced septic markers level during sepsis

I next explored the effect of Go6976 or GSK-LSD1 treatment on the regulation of inflammatory genes during sepsis. Elevation of MCP-1, IL-6, and TNF-α levels by CLP was significantly reduced in the $Lsd1^{SA/SA}$ mice (Figure III-9A), Go6976-injected or GSK-LSD1-injected mice (Figure III-9B). Systemic inflammation during sepsis frequently causes multiple organ failure, in which liver and kidney are major targeting organs (Deitch, 1992; Graetz and Hotchkiss, 2017; Shapiro et al., 2006). CLP significantly increased plasma levels of ALT (markers of hepatic injury), LDH (a marker of tissue injury), and BUN (a marker of renal injury). The concentrations of ALT, LDH, and BUN in plasma were significantly reduced in $Lsd1^{SA/SA}$ mice compared to WT mice (Figure III-9C) and were much lower in plasma of Go6976- or GSK-LSD1-injected mice than vehicle-injected mice (Figure III-9D). Our findings indicate that blocking PKCα or its downstream LSD1 activity decreases nuclear p65 protein stability thus induces resistance to acute systemic inflammation and increased survival rates during sepsis.

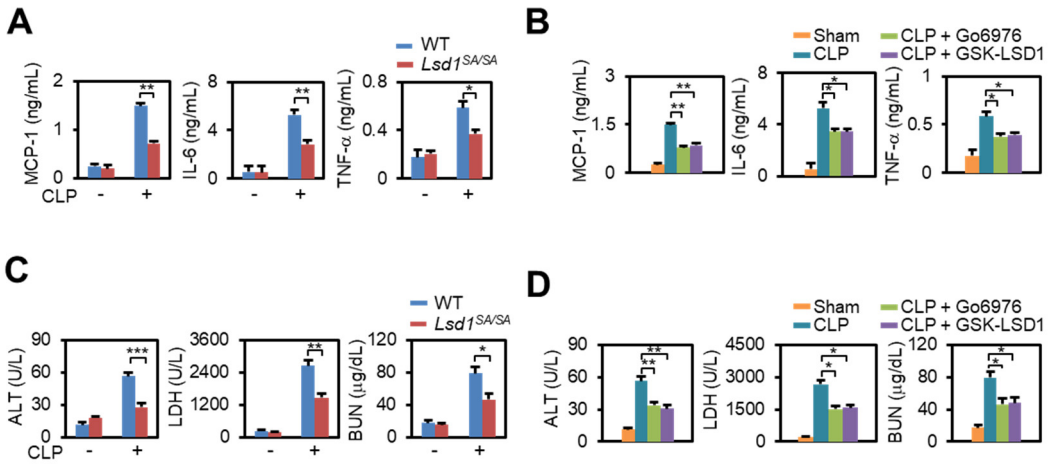

Figure III-9. *Lsd1*$^{SA/SA}$ mice, Go6976-injected or GSK-LSD1-injected mice were reduced septic markers level during sepsis

(**A** and **B**) Plasma concentrations of cytokines (MCP-1, IL-6 and TNF-α) were measured 72 hours after CLP in WT and *Lsd1*$^{SA/SA}$ mice (**A**) or in WT mice intravenously injected (1 mg/kg body weight) with Go6976 or GSK-LSD1 at 12 hours and 50 hours after CLP (**B**). (**C** and **D**) Septic injury marker (ALT, LDH and BUN) levels were measured 72 hours after CLP in WT and *Lsd1*$^{SA/SA}$ mice (**C**) or in WT mice intravenously injected (1 mg/kg body weight) with Go6976 or GSK-LSD1 at 12 hours and 50 hours after CLP (**D**). Data are expressed as Mean ± SD; n=5. *p < 0.05, **p < 0.01, ***p < 0.001 (Two-way ANOVA) (**A** and **C**). Data are expressed as Mean ± SD; n=5 per group; *p < 0.05, **p < 0.01 (unpaired two-tailed Student's *t*-test) (**B** and **D**).

III-4. Discussion

Inflammatory responses are major defense mechanisms against invading pathogens and these responses must be maintained until pathogens are cleared to avoid development of pathogen-induced diseases. On the other hands, the inflammation should be timely terminated after pathogens are removed to avoid detrimental effects caused by excessive inflammatory activations such as sepsis. Therefore, understanding the molecular mechanism of how excessive inflammatory responses are detected and maintained is necessary to alleviate sepsis-induced mortality or organ injury. In this study, I found that LSD1 phosphorylation by PKCα plays a key role in maintaining the protein stability of p65 and sustained inflammatory response following excessive LPS treatment. *In vivo* study using $Lsd1^{SA/SA}$ mice enabled us to characterize the functions of PKCα-dependent LSD1 phosphorylation in response to severe inflammation. Ablation of LSD1 phosphorylation shown in $Lsd1^{SA/SA}$ mice markedly reduced excessive inflammatory response and tissue damage upon septic shock. Also, treatment with Go6976 or GSK-LSD1 dramatically reduced excessive systemic inflammatory response, indicating that both PKCα activity and LSD1 activity are crucial for the activation of the inflammatory response.

Together with the phenotypic analyses of $Lsd1^{SA/SA}$ mice in sepsis, I demonstrate that inhibition of PKCα activity using Go6976 or LSD1 activity using GSK-LSD1 raises the survival rate with lower septic tissue injury in CLP challenge (Figure III-10). Although the treatment of antibiotics to septic patients at early stage reduces mortality, it cannot control excessive inflammatory response during septic shock. Targeting excessive inflammatory

response using the aforementioned pharmacological drugs in combination with antibiotics has potentials for the development and application to septic patients who have already been processed to systemic inflammation. Overall, our findings shed light on a potential therapeutic targeting of PKCα-LSD1-NF-κB signaling axis in inflammatory diseases.

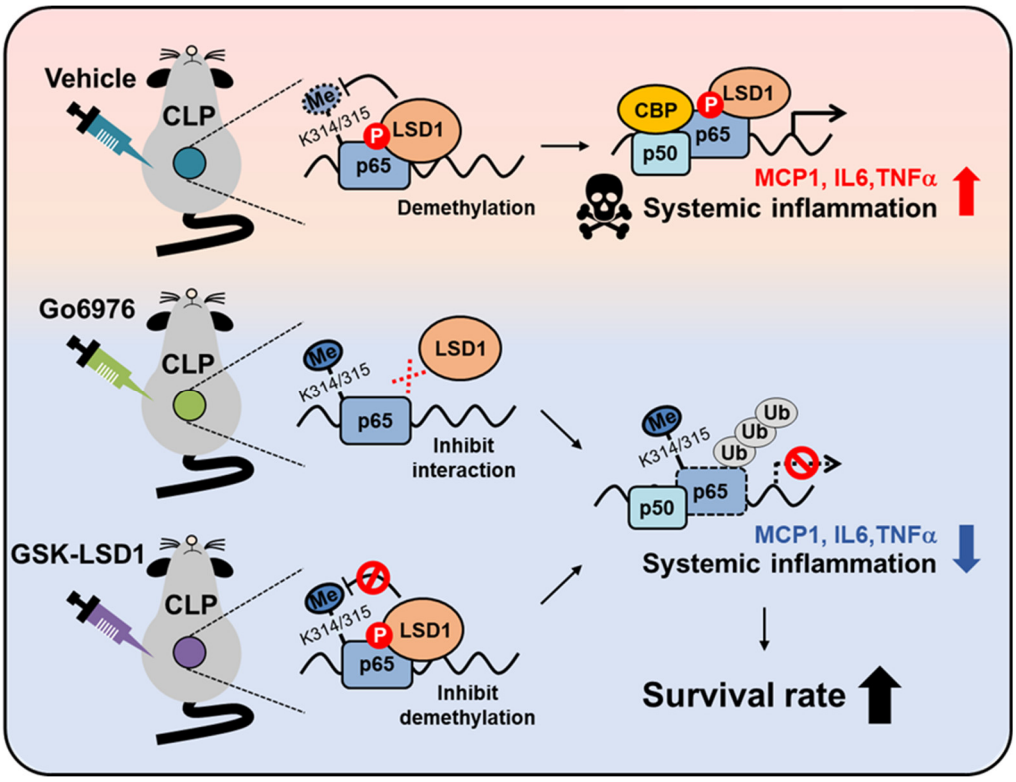

Figure III-10. Effects of mice injected with Go6976 or GSK-LSD1 after CLP

Blocking PKCα (Go6976-injected mice) or LSD1 (GSK-LSD1-injected mice) activity decreases nuclear p65 protein stability and thus increases mice survival rates in CLP-induced sepsis model.

III-5. Materials and Methods

Cell Culture

Raw264.7 (KCLB), MEFs were cultured in Dulbecco's modified Eagle's medium (DMEM, Welgene) supplemented with 10% Fetal Bovine Serum (Gibco) with ZelShield (Minerva Biolabs GmbH). To assure mycoplasma-free conditions, all cells were routinely tested.

Generation of BMDMs

Mice were sacrificed by overexposure to CO_2 anesthesia then femurs and tibias were obtained. After rinsing with 70% ethanol and cold PBS, and bone marrow was isolated from femurs and tibias. Bone marrow cells were plated at a density of 1×10^6 to 2×10^6 cells per ml in RPMI-1640 medium (Welgene) supplemented with 10% FBS (Gibco), ZelShield (Minerva Biolabs GmbH) and macrophage colony stimulating factor (10 ng/ml; Sigma, M9170) on 10 cm petri dishes and were allowed to differentiate for 7-8 days.

Antibodies and reagents

Commercially available antibodies were used: anti-p65 (sc-372, 1:1000 dilution for IB analysis), and anti-LaminA/C (sc-6215, 1:1000 dilution for IB analysis) from Santa Cruz Biotechnology; anti-LSD1 (#2139, 1:1000 dilution for IB analysis), and anti-PKCα

(#2056S, 1:1000 dilution for IB analysis) from Cell Signaling; anti-p65 (ab7970), and anti-LSD1 (ab17721), and anti-H3K9Ac (ab4441), and anti-H3K9me2 (ab1220), and anti-H3K4me2 (ab32356) from abcam; anti-LSD1 (NB-100-1762), and anti-PKCα (NB-110-57356, 1:1000 dilution for IB analysis), and anti-C/EBPδ (NB-110-85519, 1:1000 dilution for IB analysis) from NOVUS; anti-p-PKCα S657 (#06-822, 1:1000 dilution for IB analysis), and anti-p-LSD1 (ABE 1462, 1:200 dilution for IB analysis) from Millipore; anti-HA (MMS-101R, 1:5000 dilution for IB analysis) from Covance; anti-Tubulin (LF-PA0146A, 1:1000 dilution for IB analysis) from Abfrontier; anti-β-actin (A1978, 1:5000 dilution for IB analysis) from Sigma; anti-mono-methyl-p65 (K314/315) (ENH006, 1:500 dilution for IB analysis) from Elabscience Biotechnology; anti-FK2 (BML-PW8810, 1:1000 dilution for IB analysis) from Enzo Life Sciences; Lipopolysaccharides (LPS) from Escherichia coli O127:B8 (L3129), GSK-LSD1 (SML1072) from Sigma; Go6976 (13310) from Cayman; MG132 (M-1157) from A.G. Scientific; TNT T7 Quick Coupled Transcription/ Translation System (L1170) from Promega; λ-phosphatase (P0753) from NEB.

Animals

Lsd1$^{SA/SA}$ mice on the C57BL/6J background have been described (Nam et al., 2014). WT and *Lsd1*$^{SA/SA}$ male mice at 8-10 weeks of age were used in the experiments. Mice were

housed under controlled conditions of temperature (22-23°C) and light (12 hours light:12 hours dark, lights switched on at 8:00 AM). Food and water were available *ad libitum*. All animal procedures were approved by the Institutional Animal Care and Use Committee of Seoul National University.

LPS treatment

Cells were serum starved for 24 hours and treated with LPS (1 μg/ml or indicated concentration) for indicated times. Cells were lysed according to the experimental method for immunoblot analysis, quantitative RT-PCR, or ChIP assays.

Quantitative RT-PCR

Total RNA was isolated from lung tissue or BMDMs and Raw264.7 cells using TRIzol (Invitrogen). RNA was reverse-transcribed with oligo (dT) primers and M-MLV Reverse Transcriptase (Enzynomics). The obtained cDNA was mixed with TOPreal™ qPCR 2X PreMIX (SYBR Green with high ROX, Enzynomics) and gene-specific primers for PCR. The abundance of mRNA was detected by an ABI 7500 system with SYBR Green. The following primers were used:

mouse *Mcp-1* Forward 5'-GGCTCAGCCAGATGCAGTTAAC-3',

mouse *Mcp-1* Reverse 5'-AGCCTACTCATTGGGATCATCTTG-3',

mouse *Il-6* Forward 5'-CATAAAATAGTCCTTCCTACCCCAAT-3',

mouse *Il-6* Reverse 5'-CACTCCTTCTGTGACTCCAGCTTA-3',

mouse *Il-1b* Forward 5'-GATGATAACCTGCTGGTGTGTGA-3',

mouse *Il-1b* Reverse 5'-GTTGTTCATCTCGGAGCCTGTAG-3',

mouse *Cebpd* Forward 5'-CTCCACGACTCCTGCCATGT-3',

mouse *Cebpd* Reverse 5'-GAAGAGGTCGGCGAAGAGTTC-3'.

ChIP assays

Cells were cross-linked in 1 % formaldehyde for 10 min and washed with ice-cold PBS two times. Cells were collected into 1ml of harvest buffer (0.1 M Tris-HCl [pH 9.4] and freshly added 10 mM DTT) and incubated for 15 min at 30°C and centrifuged for 3 min at 6000 rpm. Cell pallets were washed sequentially with 1 ml of cold-ice PBS, buffer I (0.25 % Triton X-100, 10 mM EDTA, 10 mM HEPES [pH 6.5], and 0.5 mM EGTA) and buffer II (200 mM NaCl, 1 mM EDTA, 10 mM HEPES [pH 6.5], and 0.5 mM EGTA) and centrifuged for 3 min at 6000 rpm. Chromatin fragmentation was performed by sonication in ChIP lysis buffer (50 mM Tris-HCl [pH 8.1], 1 % SDS, 10 mM EDTA [pH 7.6] and freshly added protease inhibitor cocktail). Chromatin extracts containing DNA fragments with an average of 250 bp were then diluted ten times with dilution buffer (1 % Triton X-100, 2 mM EDTA, 150 mM NaCl, 20 mM Tris-HCl [pH 8.1] and freshly added protease

inhibitor cocktail) and subjected to immunoprecipitations overnight at 4 °C. Immunocomplexes were captured by incubating 40 µl of protein A/G sepharose for 2 h at 4 °C. Beads were washed with TSE I buffer (0.1 % SDS, 1 % Triton X-100, 2 mM EDTA, 20 mM Tris-HCl [pH 8.1] and 150 mM NaCl), TSE II buffer (0.1 % SDS, 1 % Triton X-100, 2 mM EDTA, 20 mM Tris-HCl [pH 8.1] and 500 mM NaCl), buffer III (0.25 M LiCl, 1 % NP-40, 1 % deoxycholate, 10 mM Tris-HCl [pH 8.1] and 1 mM EDTA), three times TE buffer (10 mM Tris-HCl [pH 8.0] and 1 mM EDTA) and eluted in elution buffer (1 % SDS and 0.1 M $NaHCO_3$). Crosslinking was reversed overnight at 65 °C in elution buffer, and DNA was purified with a QIAquick Gel Extraction Kit (QIAGEN). Precipitated DNA was analyzed by quantitative RT-PCR. For quantitative real-time PCR analysis, 2 µl from 50 µl DNA extractions was used. The following primers were used:

mouse *Mcp-1* Forward 5'-CACCCCATTACATCTCTTCCCC-3',

mouse *Mcp-1* Reverse 5'-TGTTTCCCTCTCACTTCACTCTGTC-3',

mouse *Il-6* Forward 5'-AGCTACAGACATCCCCAGTCTC-3',

mouse *Il-6* Reverse 5'-TGTGTGTCGTCTGTCATGCG-3'.

Preparation of tissue lysates

Lungs were rinsed with ice-cold PBS before homogenizing to remove remaining blood. Lungs were homogenized in RIPA lysis buffer (150 mM NaCl, 1 % Triton X-100, 1 %

sodium deoxycholate, 0.1 % SDS, 50 mM Tris-HCl [pH 7.5] and 2 mM EDTA [pH 8.0]) freshly supplemented with protease inhibitors. The homogenate was centrifuged (14,000 g at 4°C for 10 min), and cleared supernatant was used for immunoblot analysis.

Whole-cell lysate preparation and subcellular fractionation

All cells were briefly rinsed with ice-cold PBS before collection. For whole-cell lysates, the cells were resuspended in RIPA buffer supplemented with protease inhibitors and sonicated using a Branson Sonifier 450 at output 3 and a duty cycle of 30 for five pulses. For cytosolic and nuclear fractions, cells were lysed in buffer A (10 mM HEPES [pH 7.9], 10 mM KCl, 0.1 mM EDTA, 0.1 mM EGTA and freshly added DTT, PMSF and protease inhibitors), incubated on ice for 15 min and added 0.5 % NP-40, spun at 120 g for 1 min at 4 °C. The supernatant (cytosolic fraction) was transferred to a new tube. The nuclear pellet was rinsed twice with 500 µl of buffer A and spun down at 120 g for 1 min at 4 °C. The supernatant was discarded and the pellet (nuclear fraction) was resuspended in buffer C (20 mM HEPES [pH 7.9], 400 mM NaCl, 1 mM EDTA, 1 mM EGTA and freshly added DTT, PMSF and protease inhibitors) and sonicated as for the whole-cell lysates. All lysates were quantified by the Bradford method and analyzed by SDS–PAGE.

In vitro kinase assays

In vitro kinase assays using PKCα immunoprecipitated from HEK293T cell lysates as a kinase and purified GST-LSD1 or GST-p65 proteins as substrates were performed. PKCα and GST-LSD1 or GST-p65 were incubated at 30 °C for 30 min in kinase assay buffer (40 mM Tris-HCl [pH 7.5], 10 mM $MgCl_2$, 1 mM DTT, and 5 μCi of [γ-^{32}P] ATP). The reactions were stopped by adding 5X sample buffer and followed by boiling for 10 min. Samples were subjected to SDS-PAGE, and phosphorylation was detected by autoradiography.

In vitro GST pull-down assays

GST fusion constructs were expressed in Rosetta *E. coli* bacteria (Novagen). Crude bacterial lysates were prepared by sonication in GST binding buffer (125 mM NaCl, 20 mM Tris-HCl [pH 7.8], 10 % Glycerol, 0.1 % NP-40, 0.5 mM DTT and freshly added protease inhibitor cocktail) and lysates were centrifuged for 30 min at 13000 rpm. The supernatant was incubated with 100 μl of glutathione-Sepharose beads (GE Healthcare) at 4°C for overnight. p65 protein was generated by adding cold methionine using TNT T7 Quick Coupled Transcription/Translation system (Promega, L1170) according to the manufacture's guidance. *In vitro* kinase assay using cold ATP was performed to generate GST-LSD1 phosphorylation form before GST pull-down assay. After dividing into two

tubes, 1000 units of λ-phosphatase (NEB, P0753) were added in either phosphorylated LSD1 and incubated for 30 min at 30°C. Bead bounded GST fusion proteins were washed with buffer (150 mM NaCl, 25 mM Tris-HCl [pH 8.0], 10 % Glycerol, 0.1 % NP-40, and 1 mM EDTA) and mixed with *in vitro* transcribed/translated p65 products in GST binding buffer at 4°C for 1 hour in the presence of the protease inhibitor cocktail. The beads were washed seven times with binding buffer. The reaction beads were boiled for 10 min, then run by SDS-PAGE and analyzed by immunoblot analysis.

***In vitro* methylation and demethylation assays**

In vitro methylation assays have been described (Kim et al., 2016). Flag-p65 was purified from extracts of HEK293T cells expressing Flag-tagged p65 using Flag M2 agarose bead (Sigma, A2220). After overnight incubation at 4 °C, the beads were washed 6 times with a BC500 buffer (20 mM Tris-HCl [pH 7.9], 15 % glycerol, 1 mM EDTA, 1 mM dithiothreitol, 0.2 mM PMSF, 0.05 % Nonidet P40, and 500 mM KCl) to remove binding partners. After harsh wash, the beads were washed 3 times with a methylation assay buffer (50 mM Tris-HCl [pH 8.5], 20 mM KCl, 10 mM $MgCl_2$, 10 mM β-mercaptoethanol, and 250 mM sucrose). *In vitro* methylation assays were performed by incubating bead bound-Flag-p65 and GST-SET7/9 proteins (eluted by L-Glutathione reduced, Sigma G4251) in methylation buffer with SAM (Sigma, A7007) at 30 °C overnight. Before demethylation assay,

supernatants of assay were preserved for checking the input level of SET7/9. For *in vitro* demethylation assay, the bead-bound Flag-p65 was extensively washed with wash buffer (50 mM NaH_2PO_4 [pH 8.0], 10 mM Tris-HCl [pH 8.0], 500 mM NaCl, and 0.5 % Triton X-100) to remove remaining SET7/9 proteins, followed by addition of LSD1 protein or phosphorylated LSD1 protein obtained by *in vitro* kinase assay using clod ATP in demethylation buffer (50 mM Tris-HCl [pH 8.5], 50 mM KCl, 5 mM $MgCl_2$, 5 % glycerol, and 0.5 mM PMSF). After incubating the reaction mixtures at 37 °C for overnight, the reaction buffer was removed and 2X sample buffer were added. The reaction mixtures were boiled for 10 min, then run by SDS–PAGE and analyzed by immunoblot analysis.

Ubiquitination assays

Cells were transfected with combinations of plasmids including HisMax-tagged ubiquitin. After incubation for 48 hours, cells were treated with 5 μg/ml of MG132 for 4 hours, lysed in buffer A (6 M guanidinium-HCl, 0.1 M Na_2HPO_4/NaH_2PO_4, 0.01 M Tris-HCl [pH 8.0], 5 mM imidazole, and 10 mM β-mercaptoethanol), and incubated with Ni^{2+}-NTA beads (QIAGEN) for 4 hours at room temperature. The beads were sequentially washed with buffer A, buffer B (8 M urea, 0.1 M Na_2HPO_4/NaH_2PO_4, 0.01 M Tris-HCl [pH 8.0], and 10 mM β-mercaptoethanol), and buffer C (8 M urea, 0.1 M Na_2HPO_4/NaH_2PO_4, 0.01 M Tris-

HCl [pH 6.3], and 10 mM β-mercaptoethanol). Bound proteins were eluted with buffer D (200 mM imidazole, 0.15 M Tris-HCl [pH 6.7], 30 % glycerol, 0.72 M β-mercaptoethanol, and 5 % SDS), and subject to immunoblot analysis.

Denatured immunoprecipitation for Endogenous ubiquitination assay

Raw264.7 cells were lysed in denaturing buffer (50 mM Tris-HCl [pH 7.5], 70 mM β-Mercaptoethanol, and 1 % SDS) and boiled at 95 °C for 5 minutes. Immunoprecipitation against p65 antibody was performed after dilution with non-denaturing lysis buffer (20 mM Tris-HCl [pH 7.5], 150 mM NaCl, 1 mM EDTA, 1 mM EGTA, and 1 % Triton X-100). Samples were analyzed by immunoblotting using anti-FK2 antibody.

Immunocytochemistry assays

Lsd1$^{-/-}$ MEFs were cultured in 1 % gelatin coated coverslip. For immunocytochemistry assay, cells were washed 2 times with PBS buffer and fixed with 2 % formaldehyde for 30 min. Cells were then washed 2 times with 0.1 % Triton-X 100 in PBS (PBS-T). For permeabilization, cells were incubated in 0.5 % PBS-T for 5 min and washed 2 times with 0.1 % PBS-T. Cells were incubated in blocking solutions (5 % BSA in 0.1 % PBS-T) to

block non-specific binding of the antibody for 30 min and incubated in primary antibodies diluted in blocking solution (anti-HA, MMS-101R from Covance, 1:200 dilutions in blocking solutions; anti-p65, sc-372 from Santa Cruz, 1:200 dilutions in blocking solutions). After 8 times of washing with 0.1 % PBS-T, cells were incubated in secondary antibodies (Invitrogen, molecular probes, 1:200 dilutions in blocking solutions) and DAPI. After 8 times of washing with 0.1 % PBS-T, coverslips were mounted with vectashield (Vector laboratories) and imaged by confocal microscope (Carl Zeiss, LSM700).

Cecal ligation and puncture (CLP)

For induction of sepsis, male mice were anesthetized with 2 % isoflurane (Forane, JW pharmaceutical) in oxygen delivered via a small rodent gas anesthesia machine (RC2, Vetequip, Pleasanton), first in a breathing chamber and then via a facemask. They were allowed to breath spontaneously during the procedure. The CLP-induced sepsis was performed as described previously (Wang et al., 2004). In brief, a 2 cm midline incision was placed to allow the exposure of cecum and the adjoining intestine. The cecum was then tightly ligated using a 3.0-silk suture at 5.0 mm from the cecal tip and punctured once using a 22-gauge needle. The cecum was then gently squeezed in order to extrude a small amount of feces from perforation sites and returned to the peritoneal cavity. The laparotomy site

was then sutured with 4.0-silk. In sham control animals, the cecum was exposed but not ligated or punctured and then returned to the abdominal cavity.

Hematoxylin and eosin (H&E) staining

To analyze the phenotypic change of lung in mice, lung samples were removed from each mouse, washed 3 times in PBS to remove remaining blood, fixed in 4% formaldehyde solution (Junsei) in PBS for 20 hours at 4 °C. After fixation, the samples were dehydrated through ethanol series, embedded in paraffin, sectioned into 4 μm sections, and placed on a slide. The slides were deparaffinized in a 60 °C oven, rehydrated, and stained with hematoxylin (Sigma). To remove over-staining, the slides were quick dipped 3 times in 0.3 % acid alcohol, and counterstained with eosin (Sigma). They were then washed in ethanol series and xylene, and then cover-slipped. Light microscopic analysis of lung specimens was performed by blinded observation to evaluate pulmonary architecture, tissue edema, and infiltration of the inflammatory cells.

Clinical chemistry and cytokine level in septic mice plasma.

Fresh serum was used for assaying alanine transaminase (ALT), blood urea nitrogen (BUN),

and LDH using biochemical kits (Mybiosource). To determine the concentrations of IL-6, MCP-1 and TNF-α commercially available ELISA kits were used according to the manufacturer's protocol (R&D Systems). Values were measured using an ELISA plate reader (Tecan, GmbH).

Statistical analysis

Data were analyzed by Student's *t*-tests and log rank test for group differences, and by two-way ANOVA for condition and group differences together using GraphPad Prism software. *$p < 0.05$, **$p < 0.01$, ***$p < 0.001$.

CHAPTER IV
Conclusion

PKCα is involved in controlling the inflammatory response (Asehnoune et al., 2005; Mackay and Twelves, 2007; Silvan et al., 1996; Wang and Smart, 1999). Application of PMA, a conventional PKCs (PKCα, PKCβ1/β2, and PKCγ) agonist, to mice induces acute inflammatory response with increased expressions of the inflammatory cytokines in epidermis (Silvan et al., 1996). Although PKC signaling is shown to be crucial for the activation of inflammatory response (Asehnoune et al., 2005; Langlet et al., 2010), the molecular mechanism of activation of the inflammatory response by PKCα including downstream PKC substrates and its target genes remains unclear. LSD1 is phosphorylated by PKCα on serine 112 site and knock-in mice bearing phosphorylation-defective *Lsd1*$^{SA/SA}$ alleles show altered circadian rhythms and impaired phase resetting (Nam et al., 2014). Given a potential functional link between circadian rhythm and the inflammatory response (Curtis et al., 2014; Scheiermann et al., 2013). I speculated that *Lsd1*$^{SA/SA}$ mice might have defects not only in circadian clock physiology but also in immune response through impaired PKCα-dependent signaling. Here, I found that PKCα translocates into the nucleus and phosphorylates LSD1 after excessive inflammatory stimuli, it is tempting to speculate that PKCα functions as a sensor that links the cytoplasm and the nucleus and relays external excessive inflammatory stimuli for further activation of the inflammatory response. I demonstrate that phosphorylated LSD1 is a critical epigenetic factor for the amplification of the inflammatory response.

p65 is methylated by SET7/9 on lysine 314/315 and triggers its degradation (Yang et al., 2009a). LSD1 plays a prominent role in lysine demethylation of non-histone proteins as a counterpart of SET7/9. Here, I identify p65 as a new non-histone substrate of LSD1 and thus LSD1 is a substrate of PKCα and functions as a demethylase of p65 leading to enhanced p65 protein stability. Therefore, I demonstrate a new signaling axis of PKCα-LSD1-NF-κB in amplification of the inflammatory response following excessive inflammatory stimuli (Figure IV-1). I found that *Lsd1*$^{SA/SA}$ mice markedly reduced excessive inflammatory response and tissue damage upon septic shock. Also, treatment with Go6976 or GSK-LSD1 dramatically reduced excessive systemic inflammatory response, indicating that both PKCα activity and LSD1 activity are crucial for the activation of the inflammatory response. These data indicate that targeting PKCα-LSD1 signaling could be potentially powerful therapeutic strategy for inflammatory diseases such as sepsis.

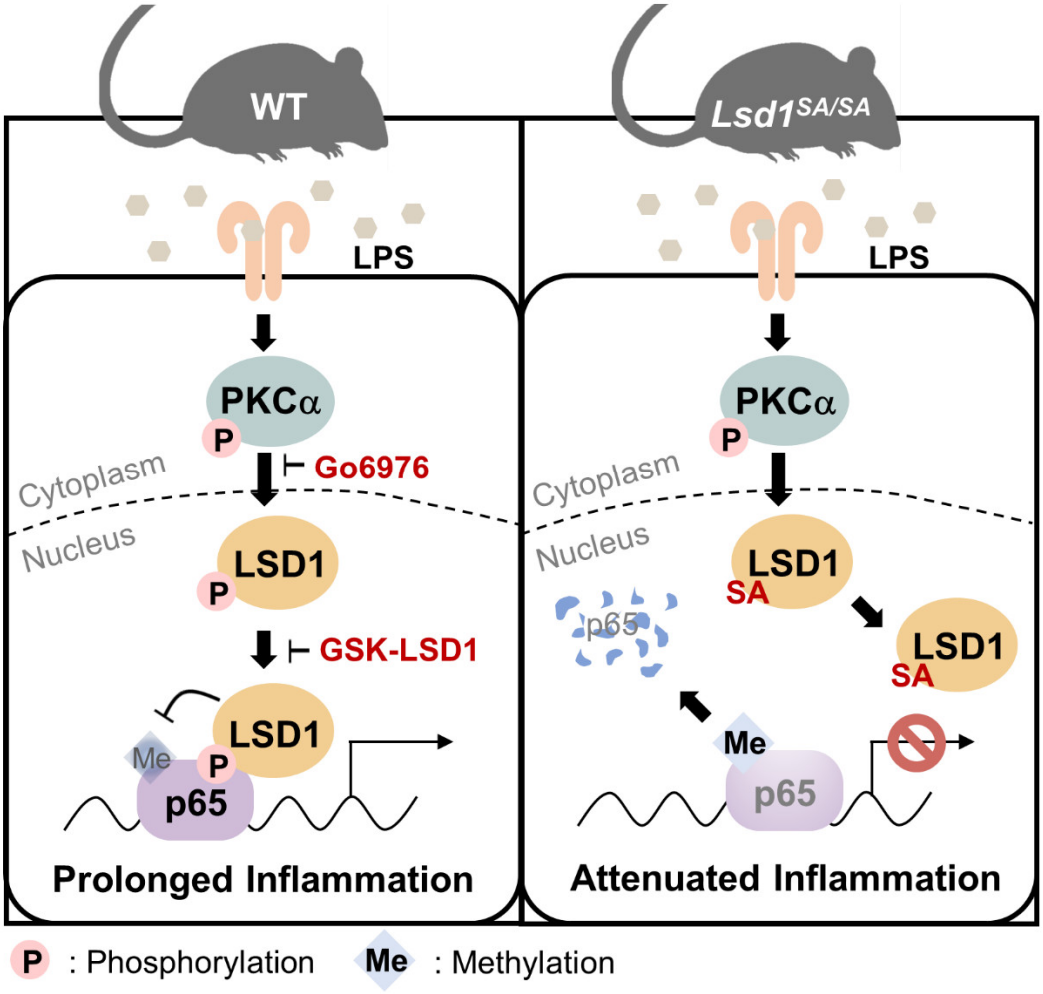

Figure IV-1. Graphical summary of the PKCα-LSD1-NF-κB signaling cascade

PKCα is translocated into the nucleus and phosphorylates LSD1 prolonged inflammatory responses (sustained inflammation) or acute septic shock. Phosphorylated LSD1 facilitates demethylation of p65 leading to enhanced p65 protein stability and stabilized p65 consistently activates NF-κB target genes. Therefore, both phosphorylation status and demethylase activity of LSD1 are required for amplification of the inflammatory response genes in NF-κB signalling.

REFERENCES

Abraham, E. (2003). Nuclear factor-κB and its role in sepsis-associated organ failure. Journal of Infectious Diseases *187*, 364-369.

Akira, S., Uematsu, S., and Takeuchi, O. (2006). Pathogen recognition and innate immunity. Cell *124*, 783-801.

Asehnoune, K., Strassheim, D., Mitra, S., Kim, J.Y., and Abraham, E. (2005). Involvement of PKCalpha/beta in TLR4 and TLR2 dependent activation of NF-kappaB. Cellular signalling *17*, 385-394.

Ashall, L., Horton, C.A., Nelson, D.E., Paszek, P., Harper, C.V., Sillitoe, K., Ryan, S., Spiller, D.G., Unitt, J.F., Broomhead, D.S.*, et al.* (2009). Pulsatile stimulation determines timing and specificity of NF-kappaB-dependent transcription. Science (New York, NY) *324*, 242-246.

Ashendel, C.L. (1985). The phorbol ester receptor: a phospholipid-regulated protein kinase. Biochimica et biophysica acta *822*, 219-242.

Basak, S., Kim, H., Kearns, J.D., Tergaonkar, V., O'Dea, E., Werner, S.L., Benedict, C.A., Ware, C.F., Ghosh, G., Verma, I.M.*, et al.* (2007). A fourth IkappaB protein within the NF-kappaB signaling module. Cell *128*, 369-381.

Basak, S., Shih, V.F., and Hoffmann, A. (2008). Generation and activation of multiple

dimeric transcription factors within the NF-kappaB signaling system. Molecular and cellular biology *28*, 3139-3150.

Bolouri, H., and Davidson, E.H. (2003). Transcriptional regulatory cascades in development: initial rates, not steady state, determine network kinetics. Proceedings of the National Academy of Sciences of the United States of America *100*, 9371-9376.

Bonizzi, G., Bebien, M., Otero, D.C., Johnson-Vroom, K.E., Cao, Y., Vu, D., Jegga, A.G., Aronow, B.J., Ghosh, G., Rickert, R.C.*, et al.* (2004). Activation of IKKalpha target genes depends on recognition of specific kappaB binding sites by RelB:p52 dimers. The EMBO journal *23*, 4202-4210.

Bours, V., Franzoso, G., Azarenko, V., Park, S., Kanno, T., Brown, K., and Siebenlist, U. (1993). The oncoprotein Bcl-3 directly transactivates through kappa B motifs via association with DNA-binding p50B homodimers. Cell *72*, 729-739.

Brantley, D.M., Chen, C.L., Muraoka, R.S., Bushdid, P.B., Bradberry, J.L., Kittrell, F., Medina, D., Matrisian, L.M., Kerr, L.D., and Yull, F.E. (2001). Nuclear factor-kappaB (NF-kappaB) regulates proliferation and branching in mouse mammary epithelium. Molecular biology of the cell *12*, 1445-1455.

Brasier, A.R. (2006). The NF-kappaB regulatory network. Cardiovascular toxicology *6*, 111-130.

Bright, R., and Mochly-Rosen, D. (2005). The role of protein kinase C in cerebral ischemic

and reperfusion injury. Stroke *36*, 2781-2790.

Buras, J.A., Holzmann, B., and Sitkovsky, M. (2005). Animal models of sepsis: setting the stage. Nature Reviews Drug Discovery *4*, 854-865.

Caamano, J., and Hunter, C.A. (2002). NF-kappaB family of transcription factors: central regulators of innate and adaptive immune functions. Clinical microbiology reviews *15*, 414-429.

Caldwell, A.B., Cheng, Z., Vargas, J.D., Birnbaum, H.A., and Hoffmann, A. (2014). Network dynamics determine the autocrine and paracrine signaling functions of TNF. Genes & development *28*, 2120-2133.

Chen, L.F., and Greene, W.C. (2004). Shaping the nuclear action of NF-kappaB. Nature reviews Molecular cell biology *5*, 392-401.

Chovatiya, R., and Medzhitov, R. (2014). Stress, inflammation, and defense of homeostasis. Molecular cell *54*, 281-288.

Curtis, A.M., Bellet, M.M., Sassone-Corsi, P., and O'Neill, L.A. (2014). Circadian clock proteins and immunity. Immunity *40*, 178-186.

Cutler, R.E., Jr., Maizels, E.T., Brooks, E.J., Mizuno, K., Ohno, S., and Hunzicker-Dunn, M. (1993). Regulation of delta protein kinase C during rat ovarian differentiation. Biochimica et biophysica acta *1179*, 260-270.

Deitch, E.A. (1992). Multiple organ failure. Pathophysiology and potential future therapy.

Annals of Surgery *216*, 117-134.

Deshmane, S.L., Kremlev, S., Amini, S., and Sawaya, B.E. (2009). Monocyte chemoattractant protein-1 (MCP-1): an overview. Journal of interferon & cytokine research *29*, 313-326.

Dev, A., Iyer, S., Razani, B., and Cheng, G. (2011). NF-kappaB and innate immunity. Current topics in microbiology and immunology *349*, 115-143.

Do-Umehara, H.C., Chen, C., Urich, D., Zhou, L., Qiu, J., Jang, S., Zander, A., Baker, M.A., Eilers, M., Sporn, P.H.*, et al.* (2013). Suppression of inflammation and acute lung injury by Miz1 via repression of C/EBP-δ. Nature immunology *14*, 461-469.

Dobrzanski, P., Ryseck, R.P., and Bravo, R. (1995). Specific inhibition of RelB/p52 transcriptional activity by the C-terminal domain of p100. Oncogene *10*, 1003-1007.

Ea, C.K., and Baltimore, D. (2009). Regulation of NF-kappaB activity through lysine monomethylation of p65. Proceedings of the National Academy of Sciences of the United States of America *106*, 18972-18977.

Feghali, C.A., and Wright, T.M. (1997). Cytokines in acute and chronic inflammation. Frontiers in bioscience : a journal and virtual library *2*, d12-26.

Feng, Z., Yao, Y., Zhou, C., Chen, F., Wu, F., Wei, L., Liu, W., Dong, S., Redell, M., Mo, Q.*, et al.* (2016). Pharmacological inhibition of LSD1 for the treatment of MLL-rearranged leukemia. Journal of hematology & oncology *9*, 24.

Foster, C.T., Dovey, O.M., Lezina, L., Luo, J.L., Gant, T.W., Barlev, N., Bradley, A., and Cowley, S.M. (2010). Lysine-specific demethylase 1 regulates the embryonic transcriptome and CoREST stability. Molecular and cellular biology *30*, 4851-4863.

Füllgrabe, J., Heldring, N., Hermanson, O., and Joseph, B. (2014). Cracking the survival code: Autophagy-related histone modifications. Autophagy *10*, 556-561.

Fuchs, S.Y., Chen, A., Xiong, Y., Pan, Z.Q., and Ronai, Z. (1999). HOS, a human homolog of Slimb, forms an SCF complex with Skp1 and Cullin1 and targets the phosphorylation-dependent degradation of IkappaB and beta-catenin. Oncogene *18*, 2039-2046.

Fusco, A.J., Huang, D.B., Miller, D., Wang, V.Y., Vu, D., and Ghosh, G. (2009). NF-kappaB p52:RelB heterodimer recognizes two classes of kappaB sites with two distinct modes. EMBO reports *10*, 152-159.

Garcia-Bassets, I., Kwon, Y.S., Telese, F., Prefontaine, G.G., Hutt, K.R., Cheng, C.S., Ju, B.G., Ohgi, K.A., Wang, J., Escoubet-Lozach, L.*, et al.* (2007). Histone methylation-dependent mechanisms impose ligand dependency for gene activation by nuclear receptors. Cell *128*, 505-518.

Gerritsen, M.E., Williams, A.J., Neish, A.S., Moore, S., Shi, Y., and Collins, T. (1997). CREB-binding protein/p300 are transcriptional coactivators of p65. Proceedings of the National Academy of Sciences of the United States of America *94*, 2927-2932.

Graetz, T.J., and Hotchkiss, R.S. (2017). Sepsis: Preventing organ failure in sepsis - the

search continues. Nature Reviews Nephrology *13*, 5-6.

Griner, E.M., and Kazanietz, M.G. (2007). Protein kinase C and other diacylglycerol effectors in cancer. Nature reviews Cancer *7*, 281-294.

Groves, R.W., Rauschmayr, T., Nakamura, K., Sarkar, S., Williams, I.R., and Kupper, T.S. (1996). Inflammatory and hyperproliferative skin disease in mice that express elevated levels of the IL-1 receptor (type I) on epidermal keratinocytes. Evidence that IL-1-inducible secondary cytokines produced by keratinocytes in vivo can cause skin disease. The Journal of clinical investigation *98*, 336-344.

Haddad, J.J., and Abdel-Karim, N.E. (2011). NF-kappaB cellular and molecular regulatory mechanisms and pathways: therapeutic pattern or pseudoregulation? Cellular immunology *271*, 5-14.

Haddad, J.J., Land, S.C., Tarnow-Mordi, W.O., Zembala, M., Kowalczyk, D., and Lauterbach, R. (2002a). Immunopharmacological potential of selective phosphodiesterase inhibition. I. Differential regulation of lipopolysaccharide-mediated proinflammatory cytokine (interleukin-6 and tumor necrosis factor-alpha) biosynthesis in alveolar epithelial cells. The Journal of pharmacology and experimental therapeutics *300*, 559-566.

Haddad, J.J., Safieh-Garabedian, B., Saade, N.E., and Lauterbach, R. (2002b). Inhibition of glutathione-related enzymes augments LPS-mediated cytokine biosynthesis: involvement of an IkappaB/NF-kappaB-sensitive pathway in the alveolar epithelium. International immunopharmacology *2*, 1567-1583.

Hah, N., Benner, C., Chong, L.W., Yu, R.T., Downes, M., and Evans, R.M. (2015). Inflammation-sensitive super enhancers form domains of coordinately regulated enhancer RNAs. Proceedings of the National Academy of Sciences of the United States of America *112*, E297-302.

Hamamoto, R., Saloura, V., and Nakamura, Y. (2015). Critical roles of non-histone protein lysine methylation in human tumorigenesis. Nature reviews Cancer *15*, 110-124.

Hatakeyama, S., Kitagawa, M., Nakayama, K., Shirane, M., Matsumoto, M., Hattori, K., Higashi, H., Nakano, H., Okumura, K., Onoe, K.*, et al.* (1999). Ubiquitin-dependent degradation of IkappaBalpha is mediated by a ubiquitin ligase Skp1/Cul 1/F-box protein FWD1. Proceedings of the National Academy of Sciences of the United States of America *96*, 3859-3863.

Hayden, M.S., West, A.P., and Ghosh, S. (2006). NF-kappaB and the immune response. Oncogene *25*, 6758-6780.

Heinz, S., Romanoski, C.E., Benner, C., Allison, K.A., Kaikkonen, M.U., Orozco, L.D., and Glass, C.K. (2013). Effect of natural genetic variation on enhancer selection and function. Nature *503*, 487-492.

Hotchkiss, R.S., and Opal, S. (2010). Immunotherapy for sepsis-a new approach against an ancient foe. New England journal of medicine *363*, 87-89.

Hotchkiss, R.S., Swanson, P.E., Freeman, B.D., Tinsley, K.W., Cobb, J.P., Matuschak, G.M.,

Buchman, T.G., and Karl, I.E. (1999). Apoptotic cell death in patients with sepsis, shock, and multiple organ dysfunction. Crit Care Med *27*, 1230-1251.

Huang, B., Yang, X.D., Lamb, A., and Chen, L.F. (2010). Posttranslational modifications of NF-kappaB: another layer of regulation for NF-kappaB signaling pathway. Cellular signalling *22*, 1282-1290.

Huang, J., Sengupta, R., Espejo, A.B., Lee, M.G., Dorsey, J.A., Richter, M., Opravil, S., Shiekhattar, R., Bedford, M.T., Jenuwein, T.*, et al.* (2007). p53 is regulated by the lysine demethylase LSD1. Nature *449*, 105-108.

Ingersoll, M.A., Platt, A.M., Potteaux, S., and Randolph, G.J. (2011). Monocyte trafficking in acute and chronic inflammation. Trends in immunology *32*, 470-477.

Inoue, M., Kishimoto, A., Takai, Y., and Nishizuka, Y. (1977). Studies on a cyclic nucleotide-independent protein kinase and its proenzyme in mammalian tissues. II. Proenzyme and its activation by calcium-dependent protease from rat brain. The Journal of biological chemistry *252*, 7610-7616.

Jacobs, M.D., and Harrison, S.C. (1998). Structure of an IkappaBalpha/NF-kappaB complex. Cell *95*, 749-758.

Jin, L., Hanigan, C.L., Wu, Y., Wang, W., Park, B.H., Woster, P.M., and Casero, R.A. (2013). Loss of LSD1 (lysine-specific demethylase 1) suppresses growth and alters gene expression of human colon cancer cells in a p53- and DNMT1(DNA methyltransferase 1)-independent

manner. The Biochemical journal *449*, 459-468.

Karin, M. (2008). The IkappaB kinase - a bridge between inflammation and cancer. Cell research *18*, 334-342.

Khansari, N., Shakiba, Y., and Mahmoudi, M. (2009). Chronic inflammation and oxidative stress as a major cause of age-related diseases and cancer. Recent patents on inflammation & allergy drug discovery *3*, 73-80.

Kim, D., Pertea, G., Trapnell, C., Pimentel, H., Kelley, R., and Salzberg, S.L. (2013). TopHat2: accurate alignment of transcriptomes in the presence of insertions, deletions and gene fusions. Genome Biology *14*.

Kim, Y., Nam, H.J., Lee, J., Park, D.Y., Kim, C., Yu, Y.S., Kim, D., Park, S.W., Bhin, J., Hwang, D.*, et al.* (2016). Methylation-dependent regulation of HIF-1alpha stability restricts retinal and tumour angiogenesis. Nat Commun *7*, doi: 10.1038/ncomms10347.

Kontaki, H., and Talianidis, I. (2010). Lysine methylation regulates E2F1-induced cell death. Molecular cell *39*, 152-160.

Kontny, E., Kurowska, M., Szczepanska, K., and Maslinski, W. (2000). Rottlerin, a PKC isozyme-selective inhibitor, affects signaling events and cytokine production in human monocytes. Journal of leukocyte biology *67*, 249-258.

Kroll, M., Margottin, F., Kohl, A., Renard, P., Durand, H., Concordet, J.P., Bachelerie, F., Arenzana-Seisdedos, F., and Benarous, R. (1999). Inducible degradation of IkappaBalpha

by the proteasome requires interaction with the F-box protein h-betaTrCP. The Journal of biological chemistry *274*, 7941-7945.

Kumar, R., Clermont, G., Vodovotz, Y., and Chow, C.C. (2004). The dynamics of acute inflammation. Journal of theoretical biology *230*, 145-155.

Lal, A., Navarro, F., Maher, C.A., Maliszewski, L.E., Yan, N., O'Day, E., Chowdhury, D., Dykxhoorn, D.M., Tsai, P., Hofmann, O.*, et al.* (2009). miR-24 Inhibits cell proliferation by targeting E2F2, MYC, and other cell-cycle genes via binding to "seedless" 3'UTR microRNA recognition elements. Molecular cell *35*, 610-625.

Langlet, C., Springael, C., Johnson, J., Thomas, S., Flamand, V., Leitges, M., Goldman, M., Aksoy, E., and Willems, F. (2010). PKC-alpha controls MYD88-dependent TLR/IL-1R signaling and cytokine production in mouse and human dendritic cells. Eur J Immunol *40*, 505-515.

Lee, M.G., Wynder, C., Cooch, N., and Shiekhattar, R. (2005). An essential role for CoREST in nucleosomal histone 3 lysine 4 demethylation. Nature *437*, 432-435.

Lim, C.S., Nam, H.J., Lee, J., Kim, D., Choi, J.E., Kang, S.J., Kim, S., Kim, H., Kwak, C., Shim, K.W.*, et al.* (2017). PKCalpha-mediated phosphorylation of LSD1 is required for presynaptic plasticity and hippocampal learning and memory. Sci Rep *7*, 4912.

Litvak, V., Ramsey, S.A., Rust, A.G., Zak, D.E., Kennedy, K.A., Lampano, A.E., Nykter, M., Shmulevich, I., and Aderem, A. (2009). Function of C/EBPdelta in a regulatory circuit

that discriminates between transient and persistent TLR4-induced signals. Nature immunology *10*, 437-443.

Liu, S.F., and Malik, A.B. (2006). NF-κB activation as a pathological mechanism of septic shock and inflammation. American Journal of Physiology Lung Cellular and Molecular Physiology *290*, L622-L645.

Liu, X.J., He, A.B., Chang, Y.S., and Fang, F.D. (2006). Atypical protein kinase C in glucose metabolism. Cellular signalling *18*, 2071-2076.

Lv, S., Bu, W., Jiao, H., Liu, B., Zhu, L., Zhao, H., Liao, J., Li, J., and Xu, X. (2010). LSD1 is required for chromosome segregation during mitosis. European journal of cell biology *89*, 557-563.

Mackay, H.J., and Twelves, C.J. (2007). Targeting the protein kinase C family: are we there yet? Nature reviews Cancer *7*, 554-562.

Mantovani, A. (2010). Molecular pathways linking inflammation and cancer. Current molecular medicine *10*, 369-373.

Medzhitov, R. (2008). Origin and physiological roles of inflammation. Nature *454*, 428-435.

Medzhitov, R., and Horng, T. (2009). Transcriptional control of the inflammatory response. Nat Rev Immunol *9*, 692-703.

Metzger, E., Wissmann, M., Yin, N., Muller, J.M., Schneider, R., Peters, A.H., Gunther, T.,

Buettner, R., and Schule, R. (2005). LSD1 demethylates repressive histone marks to promote androgen-receptor-dependent transcription. Nature *437*, 436-439.

Moscat, J., Rennert, P., and Diaz-Meco, M.T. (2006). PKCzeta at the crossroad of NF-kappaB and Jak1/Stat6 signaling pathways. Cell death and differentiation *13*, 702-711.

Muller, J., Remus, N., and Harms, K.H. (1995). Mycoserological study of the treatment of paediatric cystic fibrosis patients with Saccharomyces boulardii (Saccharomyces cerevisiae Hansen CBS 5926). Mycoses *38*, 119-123.

Mulligan, P., Yang, F., Di Stefano, L., Ji, J.Y., Ouyang, J., Nishikawa, J.L., Toiber, D., Kulkarni, M., Wang, Q., Najafi-Shoushtari, S.H.*, et al.* (2011). A SIRT1-LSD1 corepressor complex regulates Notch target gene expression and development. Molecular cell *42*, 689-699.

Munshi, N., Merika, M., Yie, J., Senger, K., Chen, G., and Thanos, D. (1998). Acetylation of HMG I(Y) by CBP turns off IFN beta expression by disrupting the enhanceosome. Molecular cell *2*, 457-467.

Murray, N.R., Baumgardner, G.P., Burns, D.J., and Fields, A.P. (1993). Protein kinase C isotypes in human erythroleukemia (K562) cell proliferation and differentiation. Evidence that beta II protein kinase C is required for proliferation. The Journal of biological chemistry *268*, 15847-15853.

Musri, M.M., Carmona, M.C., Hanzu, F.A., Kaliman, P., Gomis, R., and Parrizas, M. (2010).

Histone demethylase LSD1 regulates adipogenesis. The Journal of biological chemistry *285*, 30034-30041.

Myrick, D.A., Christopher, M.A., Scott, A.M., Simon, A.K., Donlin-Asp, P.G., Kelly, W.G., and Katz, D.J. (2017). KDM1A/LSD1 regulates the differentiation and maintenance of spermatogonia in mice. PloS one *12*, e0177473.

Nam, H.J., Boo, K., Kim, D., Han, D.H., Choe, H.K., Kim, C.R., Sun, W., Kim, H., Kim, K., Lee, H.*, et al.* (2014). Phosphorylation of LSD1 by PKCα is crucial for circadian rhythmicity and phase resetting. Molecular cell *53*, 791-805.

Natoli, G., Ghisletti, S., and Barozzi, I. (2011). The genomic landscapes of inflammation. Genes & development *25*, 101-106.

Nelson, D.E., Ihekwaba, A.E., Elliott, M., Johnson, J.R., Gibney, C.A., Foreman, B.E., Nelson, G., See, V., Horton, C.A., Spiller, D.G.*, et al.* (2004). Oscillations in NF-kappaB signaling control the dynamics of gene expression. Science (New York, NY) *306*, 704-708.

Neumann, M., and Naumann, M. (2007). Beyond IkappaBs: alternative regulation of NF-kappaB activity. FASEB journal : official publication of the Federation of American Societies for Experimental Biology *21*, 2642-2654.

Nicholson, T.B., and Chen, T. (2009). LSD1 demethylates histone and non-histone proteins. Epigenetics *4*, 129-132.

Nishizuka, Y. (1995). Protein kinase C and lipid signaling for sustained cellular responses.

FASEB journal : official publication of the Federation of American Societies for Experimental Biology *9*, 484-496.

Oeckinghaus, A., and Ghosh, S. (2009). The NF-κB family of transcription factors and its regulation. Cold Spring Harbor perspectives in biology *1*.

Otte, A.P., Kramer, I.M., and Durston, A.J. (1991). Protein kinase C and regulation of the local competence of Xenopus ectoderm. Science (New York, NY) *251*, 570-573.

Pahl, H.L. (1999). Activators and target genes of Rel/NF-kappaB transcription factors. Oncogene *18*, 6853-6866.

Perkins, N.D. (2006). Post-translational modifications regulating the activity and function of the nuclear factor kappa B pathway. Oncogene *25*, 6717-6730.

Phelps, C.B., Sengchanthalangsy, L.L., Huxford, T., and Ghosh, G. (2000). Mechanism of I kappa B alpha binding to NF-kappa B dimers. The Journal of biological chemistry *275*, 29840-29846.

Piva, R., Belardo, G., and Santoro, M.G. (2006). NF-kappaB: a stress-regulated switch for cell survival. Antioxidants & redox signaling *8*, 478-486.

Pradhan, S., Chin, H.G., Esteve, P.O., and Jacobsen, S.E. (2009). SET7/9 mediated methylation of non-histone proteins in mammalian cells. Epigenetics *4*, 383-387.

Rincon, M. (2012). Interleukin-6: from an inflammatory marker to a target for inflammatory diseases. Trends in immunology *33*, 571-577.

Robinson, M.D., McCarthy, D.J., and Smyth, G.K. (2010). edgeR: a Bioconductor package for differential expression analysis of digital gene expression data. Bioinformatics *26*, 139-140.

Rosillo, M., Sanchez-Hidalgo, M., Cardeno, A., and De La Lastra, C.A. (2011). Protective effect of ellagic acid, a natural polyphenolic compound, in a murine model of Crohn's disease. Biochemical pharmacology *82*, 737-745.

Scheiermann, C., Kunisaki, Y., and Frenette, P.S. (2013). Circadian control of the immune system. Nature Reviews Immunology *13*, 190-198.

Scoumanne, A., and Chen, X. (2007). The lysine-specific demethylase 1 is required for cell proliferation in both p53-dependent and -independent manners. The Journal of biological chemistry *282*, 15471-15475.

Semeraro, N., Ammollo, C.T., Semeraro, F., and Colucci, M. (2012). Sepsis, thrombosis and organ dysfunction. Thrombosis Research *129*, 290-295.

Shapiro, N., Howell, M.D., Bates, D.W., Angus, D.C., Ngo, L., and Talmor, D. (2006). The association of sepsis syndrome and organ dysfunction with mortality in emergency department patients with suspected infection. Ann Emerg Med *48*, 583-590.

Shi, Y., Lan, F., Matson, C., Mulligan, P., Whetstine, J.R., Cole, P.A., and Casero, R.A. (2004). Histone demethylation mediated by the nuclear amine oxidase homolog LSD1. Cell *119*, 941-953.

Shi, Y., and Whetstine, J.R. (2007). Dynamic regulation of histone lysine methylation by demethylases. Molecular cell *25*, 1-14.

Silvan, A.M., Abad, M.J., Bermejo, P., and Villar, A. (1996). Inhibition by hydroxyachillin, sesquiterpene lactone from Tanacetum microphyllum, of PMA-induced mouse ear oedema. Inflammation Research *45*, 289-292.

Smale, S.T. (2010). Selective transcription in response to an inflammatory stimulus. Cell *140*, 833-844.

Smith, A.J., Szczelkun, M.D., and Savery, N.J. (2007). Controlling the motor activity of a transcription-repair coupling factor: autoinhibition and the role of RNA polymerase. Nucleic acids research *35*, 1802-1811.

Song, X.Q., Lv, L.X., Li, W.Q., Hao, Y.H., and Zhao, J.P. (2009). The interaction of nuclear factor-kappa B and cytokines is associated with schizophrenia. Biological psychiatry *65*, 481-488.

Stahelin, R.V., Wang, J., Blatner, N.R., Rafter, J.D., Murray, D., and Cho, W. (2005). The origin of C1A-C2 interdomain interactions in protein kinase Calpha. The Journal of biological chemistry *280*, 36452-36463.

Steinberg, S.F. (2008). Structural basis of protein kinase C isoform function. Physiological reviews *88*, 1341-1378.

Takai, Y., Kishimoto, A., Inoue, M., and Nishizuka, Y. (1977). Studies on a cyclic

nucleotide-independent protein kinase and its proenzyme in mammalian tissues. I. Purification and characterization of an active enzyme from bovine cerebellum. The Journal of biological chemistry *252*, 7603-7609.

Tiruppathi, C., Soni, D., Wang, D.M., Xue, J., Singh, V., Thippegowda, P.B., Cheppudira, B.P., Mishra, R.K., Debroy, A., Qian, Z.*, et al.* (2014). The transcription factor DREAM represses the deubiquitinase A20 and mediates inflammation. Nature immunology *15*, 239-247.

Venuraju, S.M., Yerramasu, A., Corder, R., and Lahiri, A. (2010). Osteoprotegerin as a predictor of coronary artery disease and cardiovascular mortality and morbidity. Journal of the American College of Cardiology *55*, 2049-2061.

Wan, F., and Lenardo, M.J. (2009). Specification of DNA binding activity of NF-kappaB proteins. Cold Spring Harbor perspectives in biology *1*, a000067.

Wang, H., Cao, R., Xia, L., Erdjument-Bromage, H., Borchers, C., Tempst, P., and Zhang, Y. (2001). Purification and functional characterization of a histone H3-lysine 4-specific methyltransferase. Mol Cell *8*, 1207-1217.

Wang, H., Liao, H., Ochani, M., Justiniani, M., Lin, X., Yang, L., Al-Abed, Y., Wang, H., Metz, C., and Miller, E.J. (2004). Cholinergic agonists inhibit HMGB1 release and improve survival in experimental sepsis. Nature medicine *10*, 1216-1221.

Wang, H.Q., and Smart, R.C. (1999). Overexpression of protein kinase C-α in the epidermis

of transgenic mice results in striking alterations in phorbol ester-induced inflammation and COX-2, MIP-2 and TNF-α expression but not tumor promotion. Journal of cell science *112*, 3497-3506.

Wang, J., Hevi, S., Kurash, J.K., Lei, H., Gay, F., Bajko, J., Su, H., Sun, W., Chang, H., Xu, G.*, et al.* (2009). The lysine demethylase LSD1 (KDM1) is required for maintenance of global DNA methylation. Nature genetics *41*, 125-129.

Webb, B.L., Hirst, S.J., and Giembycz, M.A. (2000). Protein kinase C isoenzymes: a review of their structure, regulation and role in regulating airways smooth muscle tone and mitogenesis. British journal of pharmacology *130*, 1433-1452.

Wells, A.D. (2009). New insights into the molecular basis of T cell anergy: anergy factors, avoidance sensors, and epigenetic imprinting. Journal of immunology (Baltimore, Md : 1950) *182*, 7331-7341.

Wierda, R.J., Geutskens, S.B., Jukema, J.W., Quax, P.H., and van den Elsen, P.J. (2010). Epigenetics in atherosclerosis and inflammation. Journal of cellular and molecular medicine *14*, 1225-1240.

Wu, C., and Ghosh, S. (1999). beta-TrCP mediates the signal-induced ubiquitination of IkappaBbeta. The Journal of biological chemistry *274*, 29591-29594.

Xavier, R., and Podolsky, D. (2007). Unravelling the pathogenesis of inflammatory bowel disease. Nature *448*, 427-434.

Xiao, B., Jing, C., Wilson, J.R., Walker, P.A., Vasisht, N., Kelly, G., Howell, S., Taylor, I.A., Blackburn, G.M., and Gamblin, S.J. (2003). Structure and catalytic mechanism of the human histone methyltransferase SET7/9. Nature *421*, 652-656.

Yan, C., Johnson, P.F., Tang, H., Ye, Y., Wu, M., and Gao, H. (2013). CCAAT/enhancer-binding protein δ is a critical mediator of lipopolysaccharide-induced acute lung injury. Am J Pathol *182*, 420-430.

Yang, X.D., Huang, B., Li, M., Lamb, A., Kelleher, N.L., and Chen, L.F. (2009a). Negative regulation of NF-κB action by Set9-mediated lysine methylation of the RelA subunit. EMBO journal *28*, 1055-1066.

Yang, X.D., Lamb, A., and Chen, L.F. (2009b). Methylation, a new epigenetic mark for protein stability. Epigenetics *4*, 429-433.

Yaron, A., Hatzubai, A., Davis, M., Lavon, I., Amit, S., Manning, A.M., Andersen, J.S., Mann, M., Mercurio, F., and Ben-Neriah, Y. (1998). Identification of the receptor component of the IkappaBalpha-ubiquitin ligase. Nature *396*, 590-594.

국문 초록 / ABSTRACT IN KOREAN

염증 반응은 침입하는 병원체에 대한 숙주의 필수적인 면역방어기작이다. NF-κB 신호 전달은 염증 반응을 유도하는데 중요한 역할을 하는 것으로 가장 잘 알려져 있다. NF-κB 신호 전달의 이상이 생기면 자가 면역 질환과 같은 면역체계와 관련된 질병뿐만 아니라 각종 암 발생에도 영향을 줄 수 있다. 염증 반응의 활성화에는 protein kinase C (PKC) 신호 전달이 중요한 것으로 보고되어 있지만, PKCα에 의한 염증 반응 활성화의 영향과 관련한 분자적 기작은 아직 명확하게 밝혀져 있지 않다. 본 연구에서 PKCα가 염증 신호에 반응하여 세포질에서 세포핵 안쪽으로 이동하게 되고, LSD1을 직접 인산화 시킨다는 것을 새롭게 규명하였다. 이러한 인산화가 일어나지 않는 $Lsd1^{SA/SA}$ 마우스는 생체리듬에 이상이 생긴다는 것으로 처음 보고 되었지만, 생체리듬과 염증 반응 사이에 연관성으로 추론해 볼 때 $Lsd1^{SA/SA}$ 마우스가 면역 반응에서도 이상이 나타날 수 있을 것이라고 예측하고 LSD1 인산화의 면역학적 조절기전 연구를 진행하였다.

p65는 염증 반응과 관련한 NF-κB 신호 전달체계에서 가장 중요한 전사인자이다. p65는 Lipopolysaccharide (LPS)라는 면역 신호에 반응하여 면역 반응에 관여하는 사이토카인 등의 유전자 발현에 직접 작용한다. 따라서 p65의 기능을 조절할 수 있는 기전 연구는 면역 질환에 대한 이해에 있어서 매우 중요하다. 본 연구에서 LPS에 의해서 유도되어 핵 안으로 들어온 PKCα를 통해 인산화된 LSD1만이 p65와 직접적으로 결합할 수 있다는 것을 확인하였다. 인산화된 LSD1과 결합한 p65는 LSD1의 활성에 의해서 탈메틸화가 유도되어 단백질이 안정화 되고, p65의 안정화를

통한 지속적인 target 유전자의 발현이 나타나는 것을 확인할 수 있었다. 따라서 LSD1의 인산화 조절을 통하여 p65의 기능에 영향을 주어 염증 반응 자체를 조절할 수 있다는 것을 새롭게 밝혔다.

본 연구를 통해서 PKCα-LSD1-NF-κB의 신호전달 축을 제시하여 과도한 면역 자극 신호에 의해서 증폭되고 유지되는 염증 반응의 새로운 기작을 규명하였다. 이러한 내용은 $Lsd1^{SA/SA}$ 마우스가 패혈증 상황에서 과도한 염증 반응에 의한 조직손상이 적게 나타나고, 생존율이 증가하는 양상을 통해서도 증명할 수 있었다. 또한 Go6976 또는 GSK-LSD1의 PKCα와 LSD1 저해제를 주사한 마우스의 실험에서도 $Lsd1^{SA/SA}$ 마우스와 마찬가지로 조직손상 저해와 생존율의 증가가 비슷하게 나타나는 것으로도 확인할 수 있었다. 이번 연구결과를 토대로 염증 반응에서 PKCα-LSD1 신호전달의 조절은 향후 패혈증과 같은 과도한 염증 반응에 의한 면역 질환에 잠재적인 치료약물 후보로도 중요하게 부각될 수 있는 가능성을 제시할 수 있다.

주요어:

LSD1, PKCα, 인산화, 후성유전학적 조절, NF-κB, p65, C/EBPs, 전사 조절, LPS, 염증 반응, 패혈증

학번: 2010-20306